

# **Stony Brook University**



OFFICIAL COPY

**The official electronic file of this thesis or dissertation is maintained by the University Libraries on behalf of The Graduate School at Stony Brook University.**

**© All Rights Reserved by Author.**

**Regenerating the Mammalian Heart: Potential Roles for  
Cardiomyocyte Proliferation, Cardiac Stem Cells, and Fibroblasts**

A Dissertation Presented

by

**Adam Jerome Thibodeau Schuldt**

to

The Graduate School

in Partial Fulfillment of the

Requirements

for the Degree of

**Doctor of Philosophy**

in

**Biomedical Engineering**

Stony Brook University

May 2008

Copyright by  
**Adam Jerome Thibodeau Schuldt**  
**2008**

**Stony Brook University**

The Graduate School

**Adam Jerome Thibodeau Schuldt**

We, the dissertation committee for the above candidate for the

Doctor of Philosophy degree,

hereby recommend acceptance of this dissertation.

**Ira S. Cohen, M.D., Ph.D., Dissertation Advisor**

Leading Professor, Department of Physiology and Biophysics  
Stony Brook University

**Emilia Entcheva, Ph.D., Chairperson of Defense**

Associate Professor, Department of Biomedical Engineering  
Stony Brook University

**Peter R. Brink, Ph.D.**

Professor and Chairman, Department of Physiology and Biophysics  
Stony Brook University

**Glenn R. Gaudette, Ph.D.**

Assistant Professor, Department of Biomedical Engineering  
Worcester Polytechnic Institute

This dissertation is accepted by the Graduate School

Lawrence Martin  
Dean of the Graduate School

Abstract of the Dissertation

**Regenerating the Mammalian Heart: Potential Roles for Cardiomyocyte Proliferation,  
Cardiac Stem Cells, and Fibroblasts**

by

Adam Jerome Thibodeau Schuldt

Doctor of Philosophy

in

Biomedical Engineering

Stony Brook University

2008

The human heart has long been considered a postmitotic organ which is unable to regenerate contractile cells. Recent evidence has challenged this notion, indicating that the heart does regenerate cardiomyocytes, but at a rate too slow to be therapeutic in a setting of heart disease. A large body of recent work has aimed to increase the rate of cardiomyocyte replacement to therapeutic levels. Most of this research has focused on the potential of various types of stem cells to reconstitute the diseased heart, with some evidence even suggesting the existence of resident cardiac stem cells. However, a second source of cardiac regeneration may reside in the proliferation of adult cardiomyocytes. The present body of work represents investigations into both of these approaches. Our laboratory has shown that human mesenchymal stem cells (hMSCs) can stimulate adult cardiomyocytes to proliferate *in vitro*. Based on our results and the

work of others, we hypothesized that paracrine factors from the stem cells may permit cardiomyocyte re-entry into the cell cycle. Co-cultures of adult canine cardiomyocytes and hMSCs or hMSCs transfected with the genes that encode proteins relevant to cardiomyocyte proliferation were employed to investigate the role of paracrine signaling. The use of transfected hMSCs and growth factor supplementation was shown to augment the rate of colony formation in cardiomyocyte cultures. However, while the rate of cardiomyocyte proliferation may have increased, it still remained below the levels of detection using time-lapse microscopy.

Stemming from our research on colony formation, the source of cells described by others as resident cardiac progenitor cells and implicated in the formation of three-dimensional aggregates termed “cardiospheres” was investigated. Our results suggest that the cardiospheres are comprised primarily of fibroblasts, rather than a population of rapidly proliferating resident cardiac stem cells. Further experiments showed that similar spheroid structures could be created from fibroblasts derived from other tissue sources. *In vitro* differentiation protocols confirm that cells from these spheres can differentiate along a cardiac lineage, as well as other mesenchymal cell types including adipose, bone, and cartilage.

# Table of Contents

<b>LIST OF FIGURES .....</b>	<b>vi</b>
<b>1 BACKGROUND AND SIGNIFICANCE.....</b>	<b>1</b>
1.1 PATHOPHYSIOLOGY OF HEART FAILURE AND MYOCARDIAL INFARCTION.....	1
1.2 CHANGING ATTITUDES IN CARDIOLOGY .....	1
1.3 TWO STRATEGIES OF CARDIAC REGENERATION: DIFFERENTIATION OF STEM CELLS AND PROLIFERATION OF MATURE CARDIOMYOCYTES.....	2
1.4 EPIDEMIOLOGY AND TREATMENT OF HEART DISEASE .....	3
<b>2 OVERVIEW OF RESEARCH FINDINGS.....</b>	<b>5</b>
<b>3 RESEARCH FINDINGS .....</b>	<b>6</b>
3.1 PARACRINE FACTORS FROM hMSCs MAY STIMULATE CARDIOMYOCYTE PROLIFERATION .....	6
3.1.1 <i>Introduction</i> .....	6
3.1.2 <i>Methods</i> .....	7
3.1.3 <i>Results</i> .....	10
3.1.4 <i>Discussion</i> .....	24
3.2 CARDIOSPHERES ARE DERIVED FROM FIBROBLASTS.....	27
3.2.1 <i>Introduction</i> .....	27
3.2.2 <i>Methods</i> .....	29
3.2.3 <i>Results</i> .....	33
3.2.4 <i>Discussion</i> .....	82
<b>4 REFERENCES .....</b>	<b>88</b>

## List of Figures

<b>FIGURE 1.</b> EXPRESSION OF Wnt5A PROTEIN IN hMSCs TRANSFECTED WITH A Wnt5A PLASMID. ....	11
<b>FIGURE 2.</b> COLONY FORMATION IN CO-CULTURES OF CANINE CARDIAC MYOCYTES AND hMSCs SEPARATED BY A POROUS MEMBRANE. ....	13
<b>FIGURE 3.</b> MORPHOLOGICAL ALTERATIONS AND STAINING OF CARDIAC MYOCYTES IN CO-CULTURE WITH Wnt5A-hMSCs.....	15
<b>FIGURE 4.</b> COMPARISON OF COLONY FORMATION IN Wnt5A-hMSC + IGF-1 CO-CULTURES WITH Wnt5A-hMSC ALONE, hMSC + IGF-1, AND hMSC CO-CULTURE ALONE. ....	18
<b>FIGURE 5.</b> LARGE SPHERICAL COLONIES OF FIBROBLAST-LIKE CELLS IN A CARDIAC MYOCYTE CULTURE. ....	20
<b>FIGURE 6.</b> NUMBER OF CARDIAC MYOCYTE COLONIES FORMED AFTER INCUBATION WITH A-FSP ANTIBODY IN EACH OF TWO SEPARATE EXPERIMENTS. ....	22
<b>FIGURE 7.</b> PHASE-BRIGHT CELLS (ARROWHEADS INDICATE SOME EXAMPLES) FROM A CANINE LV MID-MYOCARDIUM EXPLANT IMAGED ON CULTURE DAY 13 .....	34
<b>FIGURE 8.</b> TIME-LAPSE IMAGES FROM A CANINE LEFT VENTRICULAR MID-MYOCARDIUM EXPLANT CULTURE.. ....	36
<b>FIGURE 9.</b> REPRESENTATIVE IMAGES SHOWING THE FORMATION OF SPHERES FROM CRV FIBROBLASTS OVER TIME.....	39
<b>FIGURE 10.</b> SPHERE FORMATION AT DAY 3 USING PHASE-BRIGHT CELLS WASHED OFF OF THE EXPLANT PLATE VERSUS FIBROBLASTS COLLECTED BY TRYPSINIZATION.. ....	41
<b>FIGURE 11.</b> TIME-LAPSE IMAGES OF A CANINE DERMAL EXPLANT CULTURE. ....	44
<b>FIGURE 12.</b> FIBROSPHERE FORMATION FROM CANINE DERMAL-DERIVED CELLS.. ....	46
<b>FIGURE 13.</b> TIME-LAPSE IMAGES OF PORCINE RV EXPLANTS.....	50
<b>FIGURE 14.</b> CARDIOSPHERES AND DERMAL FIBROSPHERES DERIVED FROM PORCINE TISSUE.....	52
<b>FIGURE 15.</b> “SURVIVAL ANALYSIS” OF CANINE VERSUS PORCINE DERMAL PHASE-BRIGHT CELLS.....	54
<b>FIGURE 16.</b> TIME-LAPSE IMAGES FROM A HUMAN RA EXPLANT CULTURE .....	57
<b>FIGURE 17.</b> FIBROSPHERE FORMATION WITH NHLFs.....	60
<b>FIGURE 18.</b> CARDIAC DIFFERENTIATION OF CARDIOSPHERE-DERIVED CELLS.....	62
<b>FIGURE 19.</b> CHONDROGENIC DIFFERENTIATION OF CANINE CARDIOSPHERE-DERIVED CELLS. ....	65
<b>FIGURE 20.</b> OSTEOGENIC DIFFERENTIATION OF CANINE RIGHT VENTRICULAR CDCs.....	67
<b>FIGURE 21.</b> DIFFERENTIATION OF CANINE DERMAL FDCs INTO FAT AFTER ADIPOGENIC INDUCTION.....	70
<b>FIGURE 22.</b> CHONDROGENIC DIFFERENTIATION OF CANINE DERMAL FDCs.....	72
<b>FIGURE 23.</b> CARDIOMYOCYTE DIFFERENTIATION OF CANINE RV-DERIVED CFCS .....	76
<b>FIGURE 24.</b> OSTEOGENIC DIFFERENTIATION OF CANINE DERMAL FFCs AND FDCs .....	78
<b>FIGURE 25.</b> ADIPOGENIC DIFFERENTIATION RESULTS FROM NHDFs CULTURED WITH OR WITHOUT FIBRONECTIN AND EXPOSURE TO GROWTH FACTORS. OIL RED-O STAINED IMAGES.....	80



## Acknowledgements

My development as a research scientist is owed entirely to the superb mentoring I have received throughout the years since I was an undergraduate, and indeed even before. First and foremost, a great deal of gratitude goes out to the members of my dissertation committee—Drs. Ira Cohen, Emilia Entcheva, Glenn Gaudette, and Peter Brink. During my graduate training I have been extremely fortunate to have had the opportunity and privilege to learn from and work with Ira Cohen. As an advisor, he has been exceptional and has truly provided an example by which I can only hope to model my own interactions with students in the future. As a scientist, his creativity and insight have provided inspiration for my own research endeavors, pushing me to recognize the less obvious applications for both novel findings and well-established knowledge. His dedication to preparing students for each stage of their training and (more importantly) success in their future careers makes him admirable as a mentor, while his willingness to go the extra distance to help in matters outside of the laboratory makes him a true friend.

A lot of credit and thanks go to Emilia Entcheva for contributing invaluable experience and thoughtful suggestions to this work, in addition to providing the cells and facilities which allowed me to perform the experiments with rat neonatal ventricular myocytes. Without her assistance, this research would not have been possible. I have also been fortunate to benefit from her excellent teaching abilities in a course which provided me with the knowledge and understanding of microscopy techniques required to image and analyze the histological samples shown throughout this dissertation. Glenn Gaudette has been a wonderful teacher and a great resource for knowledge and ideas in all of our collaborations together. His energy and enthusiasm for instructing and contributing to science is unique, and it is an example of what to strive for in my own career. Peter Brink provided helpful advice on the histological work performed in these experiments, as well as thoughtful comments on the data collected throughout the course of this research. I also owe a tremendous debt of gratitude to Peter and Ira for their strong support in helping make the next move in my personal and professional life a reality.

A large number of people contributed their efforts to the experiments described in this dissertation. The foundation for the experiments described in Chapter 3.1 was formed from work produced by Sergey Doronin on the effects of stem cell co-culture and Wnt5a expression on cardiomyocyte proliferation. Cardiomyocyte preparations were prepared by Joan Zuckerman and Chris Gordon, while Joan also assisted in preparation of tissue explants for the experiments in Chapter 3.2. Irina Potopova developed the ELISA protocol used to evaluate Wnt5a expression and assisted with cell

cultures when needed. Many thanks are owed to Mark Bowen for his generosity in allowing us to use his time-lapse microscope for imaging the appearance and disappearance of the phase-bright cells described in Chapter 3.2. The adipogenic, chondrogenic, and osteogenic differentiation protocols in the same chapter were performed by Yuanjian Guo, while the rat neonatal ventricular myocyte preparations for cardiogenic differentiation were prepared by Chiung-Yin Chung and Sunita Chugh in Emilia Entcheva's laboratory. Additional thanks go to the rest of the Entcheva laboratory for help with feeding the neonatal rat ventricular myocytes cultures.

Also, many thanks go out to my fellow graduate students in Ira's laboratory, Amy Rosen, Damon Kelly, Victor Tselentakis, Jia Lu, and Ling Li. Their camaraderie made this experience truly enjoyable, and I am fortunate to be able to count them not only as colleagues, but also as friends. In particular, Amy, Damon, and Victor provided excellent suggestions on experimental design and interpretation of data, as well as life-saving assistance with Biomedical Engineering concepts and MATLAB programming, all of which were new to me when I entered this program.

I also owe great debts of gratitude to Dr. Beverly Lorell for the excellent training I received while working for her at Harvard Medical School, and Drs. Jane Barker and Brian Soper for two years of terrific experiences at the Jackson Laboratory. Drs. Amy Johnson and Patsy Dickinson at Bowdoin College provided my earliest experiences in biological research, which first inspired me to consider research as a possible career.

Since long before I decided I wanted to become a physician in the 7<sup>th</sup> grade, my family has provided tremendous love and support. Without the encouragement of my parents, Marcia and Jerry, who instilled in me from the beginning the value of an education and the rewards of hard work, I could not have made it this far. They never protested when my path took me far from home and have always given me the freedom to learn, experience, and grow. My brothers, Nathan and Tyler, and sisters, Sara and Megan, have always believed in me, and each one's desire to follow his or her own dreams while maintaining balance in their lives has served as a frequent reminder to me to do the same.

Since the beginning of my time at Stony Brook, one person has been a constant pillar of support and a beacon of sunshine in the windowless halls of the Health Science Center. My wonderful fiancée, Waitz Ngan, has been a helpful study partner, an unwavering friend, an endless source of love and respect, and a caring hand when I was too caught up in lab work to remember to eat. She has provided wonderful companionship every day, put up with me when failed experiments made me irritable, and celebrated with me during moments of success. She and her parents have welcomed me into their family with warmth and generosity, and for that I am most grateful.

# 1 Background and Significance

## 1.1 Pathophysiology of Heart Failure and Myocardial Infarction

Cardiac insults such as myocardial infarction (MI) or chronic pressure or volume overload ultimately lead to the loss of the heart's contractile cells—the cardiomyocytes. The heart responds to such challenges by compensatory mechanisms which include hypertrophic growth of the existing myocytes (adding sarcomeres in series in the case of volume overload or in parallel in pressure overload), rather than hyperplasia, or the generation of new contractile cells. Over time, the increased work load on the remaining cells causes them to deteriorate. The continuing loss of cardiomyocytes causes a thinning of the heart wall and a decrease in the heart's ejection fraction (the fraction of blood volume in the heart at end diastole that is ejected during contraction). The larger blood volume remaining in the heart combined with the thinner wall increase wall stress. This causes the heart chamber to dilate as the cells continue to add sarcomeres in series. While this response may serve to decrease wall stress temporarily, it also further decreases the heart's pumping efficiency, leading to increased volume overload. Over time, the cycle of cell loss, increased wall stress, and increased demands on the remaining cells causes the heart function to spiral downward, ultimately reaching a state of heart failure. By the time left ventricular (LV) heart failure has been reached, it is estimated that between 1 and 1.7 billion myocytes have been lost, corresponding to a loss of 25-30% of the LV tissue.<sup>1, 2</sup> Given the heart's natural tendency to favor hypertrophy of existing cells and scar formation in infarcted areas over hyperplasia, it has long been thought that the heart is incapable of regenerating contractile cells to effectively repair itself.

## 1.2 Changing attitudes in Cardiology

In recent years, evidence has mounted in support of the notion that the heart may be capable of producing new myocytes, challenging the long-held belief that the heart is a post-mitotic organ. The initial report by Orlic, et al.<sup>3</sup> that demonstrated regeneration of cardiomyocytes, endothelium, and smooth muscle from c-kit<sup>+</sup> bone marrow cells in the infarcted mouse heart opened the field of cardiac regeneration. This was followed by the discovery of host-derived cardiomyocytes in the donor hearts of sex-mismatched transplant patients.<sup>4-7</sup> These findings suggested that adult humans maintained a population of cells with the capacity to differentiate along a cardiac lineage. This finding has generated new hope for improved therapeutic options for

heart disease patients which focus on replacing lost cardiac cells, rather than relying on pharmacologic agents which aim to slow disease progression or simply treat symptoms. Other evidence would later suggest that fusion of the implanted stem cells to cardiomyocytes might explain the presence of cardiac lineage-specific markers on the delivered stem cells.<sup>8</sup> Notwithstanding this possibility, the observation that apoptosis can be observed in the adult heart at any age implies that cardiomyocyte regeneration is necessary to maintain cardiac mass throughout adulthood.<sup>9</sup> Identification and exploitation of the mechanism(s) involved in this cellular homeostasis in the heart could have enormous therapeutic potential.

### *1.3 Two strategies of cardiac regeneration: differentiation of stem cells and proliferation of mature cardiomyocytes*

In principle, there are two main routes by which cardiomyocytes could be regenerated: 1) a population of progenitor (stem) cells could exist which can differentiate into cardiomyocytes and 2) cardiomyocytes could re-enter the cell cycle and proliferate. The reports of bone marrow-derived cardiomyocytes in the mouse and host-derived cardiomyocytes in human transplant patients stimulated several investigations into the potential of bone marrow cells to become cardiomyocytes. Although attempts by other groups to reproduce the initial findings of Orlic, et al. in the mouse failed,<sup>10, 11</sup> other research supported the idea that certain subpopulations of bone marrow-derived cells have the potential to implant in the heart and differentiate along a cardiac lineage. Investigations using mesenchymal stem cells (MSCs) from the bone marrow have been encouraging.<sup>12</sup> These cells have been successfully differentiated along a cardiac lineage *in vitro* using 5-azacytidine.<sup>13, 14</sup> Injection of MSCs has demonstrated differentiation of MSCs to express cardiac-specific markers and phenotype<sup>15</sup> as well as improved cardiac function in postinfarction models.<sup>16, 17</sup> A body of recent work has also described the existence of stem cells which reside within the heart itself, and some of this research will be the focus of Chapter 3.2 of this dissertation.

Additional efforts have focused on endogenous cardiomyocyte proliferation. Anversa's group first reported increased cardiomyocyte mitoses in human patients with end-stage heart failure in 1998<sup>18</sup> and with myocardial infarction in 2001.<sup>19</sup> Several studies have attempted to establish baseline values for the mitotic indexes in the healthy and diseased heart, but the results have varied tremendously within a given species.<sup>20</sup> Whatever the actual rate, it was generally believed that cardiomyocyte proliferation did not play a significant role in cardiac injury repair. In 2002, Keating et al.

demonstrated apparently complete regeneration following surgical excision of 20% of the ventricle of the zebrafish and showed that cardiomyocyte proliferation was the primary mechanism.<sup>21</sup> This raised the question whether this represented a more primitive characteristic of cardiomyocytes that could be reactivated in humans. Investigators have since been seeking ways to induce cardiomyocyte proliferation in mammals. Several papers have identified genes or molecules that may play a regulatory role, including members of the HAND transcription factor family and the growth factors FGF, IGF, and EGF.<sup>20</sup> One report demonstrated that simply increasing the capillary bed in an infarct by injection of angioblast cells resulted in a five-fold increase in cardiomyocyte proliferation in the rat.<sup>22</sup>

#### *1.4 Epidemiology and treatment of heart disease*

Heart disease is the number one cause of death in men ages 40-54 and in both men and women over age 75 and is second only to malignancy in men ages 55 to 74.<sup>23</sup> Coronary heart disease (CHD) afflicts 13,000,000 Americans; of them, 7.1 million have had a myocardial infarction.<sup>24</sup> It was estimated that 700,000 Americans would suffer their first coronary attack in 2006;<sup>24</sup> the average age of first heart attack for men is 65.8 years, while it is 70.4 for women.<sup>24</sup> Coronary heart disease carries a 49% lifetime risk after age 40 in men, and a 32% risk after 40 for women.<sup>24</sup> CHD is the single largest killer of men and women in this country, accounting for one of every five deaths.<sup>24</sup> The financial burden of CHD was expected to add up to \$142.1 billion for 2005.<sup>24</sup>

Congestive heart failure (CHF) has a nation-wide prevalence of 4,900,000<sup>24</sup> and carries a 5 year mortality rate of 59% in men and 45% in women;<sup>25</sup> the one year mortality rate is 20%.<sup>24</sup> Due to the aging US population, an increase in the incidence of coronary heart disease and heart failure is expected.<sup>26</sup> Even at the current incidence of 550,000 new cases per year, an estimated \$28 billion will be spent on management of CHF this year.<sup>24</sup> The total deaths from CHF increased 35.3% from 1992 to 2002.<sup>24</sup> At age 40, the lifetime risk of developing CHF is 20% for both men and women.<sup>24</sup> Total mortality due to CHF in 2001 was 264,900.<sup>24</sup>

The current standard of treatment for CHF relies on titrating a delicate balance of pharmacologic agents in an attempt to prevent cardiac hypertrophy and remodeling. This includes drugs which reduce peripheral vascular resistance (vasodilators), reduce the circulatory volume (diuretics), and inhibit the renin-angiotensin-aldosterone system (ACE inhibitors, aldosterone antagonists). Treatment is complicated by the need to determine if and when it is appropriate to decrease contractility by employing a gradual blockade of  $\beta$ -adrenergic receptors in the heart ( $\beta$ -blockers) or administration of

contractility-enhancing drugs such as  $\beta$ -adrenergic agonists or digitalis in each individual patient. Once the disease progresses to the point where these treatments are no longer effective, patients must undergo drastic procedures including, but not limited to, long-term implantation of a mechanical assist device or even heart transplantation. Unfortunately, only 2,192 heart transplant procedures were performed in 2006 in the US,<sup>27</sup> due to limited organ availability. These procedures have important long-term complications which must be monitored and treated. Despite all of the efforts of physicians, the best most patients can hope for is adequate management to delay the progression of their disease, as no cure for heart failure (outside of transplantation) currently exists.

## 2 Overview of Research Findings

The present body of work describes experiments investigating two different approaches to the goal of replacing cardiomyocytes lost in heart disease. The first set of experiments involves an attempt to use paracrine factors to increase the rate of cardiomyocyte proliferation. The second set examines the source of cells described by others as cardiac stem cells and implicated in the formation of cardiospheres.<sup>28, 29</sup>

**Chapter 3.1** – Co-culture of adult canine cardiomyocytes with Wnt5a-overexpressing human mesenchymal stem cells (Wnt5a-hMSCs) separated by a porous membrane and supplemented with insulin-like growth factor 1 (IGF-1) was employed to induce proliferation of the cardiomyocytes. A large increase in cardiomyocyte colony formation was observed in these cultures compared with co-culture with plain hMSCs alone. However, cardiomyocyte proliferation could not be observed in time-lapse images of the cultures. Therefore, while the rate of proliferation may have been increased, it still remained too low to be detected by the methods used here.

**Chapter 3.2** – The “phase-bright” cells described by Messina et al. and Smith et al. were shown to arise from the monolayer of fibroblasts growing out from cardiac explants. These phase-bright cells appear to simply represent fibroblasts undergoing mitosis. Explants of dermal, aortic, and brain tissue also produced phase-bright cells in the same manner. Fibroblasts collected from cardiac explants produced “cardiospheres,” while fibroblasts from the other tissues studied produced analogous “fibrospheres.” Furthermore, the cells derived from the spheres, as well as those that form the spheres, showed an ability to differentiate along cardiac, adipose, bone, and cartilage lineages.

## 3 Research Findings

### 3.1 *Paracrine factors from hMSCs may stimulate cardiomyocyte proliferation*

#### 3.1.1 Introduction

Evidence from our laboratory suggests that paracrine factors may be capable of stimulating adult cardiomyocytes to dedifferentiate and proliferate. We have previously demonstrated that hMSCs, when co-cultured with adult canine cardiomyocytes, could stimulate formation of myocyte colonies.<sup>30</sup> This finding was accompanied by positive staining for cyclin D1 in the nuclei of the cardiomyocytes. A 2004 study demonstrated that paracrine factors from embryonic stem cells could correct deficient myocardium development in a knock-out model of a thin-walled heart.<sup>31</sup> The results from this study further suggested that Wnt5a and insulin-like growth factor 1 (IGF-1) may be key paracrine factors involved in this recovery of cardiomyocyte development. Preliminary evidence from our laboratory indicates that overexpression of Wnt5a in hMSCs can augment the degree of adult cardiomyocyte proliferation in co-culture, membrane-separated culture, and media exchange experiments. Therefore, we set out to investigate whether addition of IGF-1 to the Wnt5a-conditioned media may result in formation of greater numbers of cardiomyocyte colonies in membrane-separated co-cultures with Wnt5a-expressing hMSCs.

To examine this question, hMSCs were transfected with a gene encoding the Wnt5a protein (Wnt5a-hMSCs) and plated on a porous membrane. Adult canine cardiomyocyte cultures were established, and the membranes with Wnt5a-hMSCs were placed in the cardiomyocyte cultures, establishing two separate cell compartments which were able to share media. The cells were fed using media supplemented with IGF-1, and the formation of colonies of cardiomyocytes over time was quantified.

The ability to use paracrine factors to stimulate cardiac regeneration would open the door to two potential therapeutic modalities: *in vitro* expansion of a deliverable population of cells with cardiogenic potential, or *in vivo* delivery of paracrine factors via cells or solutions to promote *in situ* cardiomyocyte proliferation. Both of these options could effectively bypass the difficulties encountered with heterologous stem cell therapies by expanding the patient's own cardiomyocytes either in culture or in the heart itself.



### **3.1.2 Methods**

#### **Preparation of Wnt5a Plasmid**

Wnt5a plasmid was expanded in *Escherichia coli* using the Max Efficiency DH10B Competent Cell kit from Invitrogen (Carlsbad, CA). The plasmid contains an ampicillin resistance gene downstream from the Wnt5a gene. Transfected *E. coli* were streaked on agarose plates containing 100 µg/ml ampicillin and placed in a 37°C incubator. A single colony was isolated and inoculated into LB broth containing 50 µg/ml ampicillin and incubated at 37°C on an orbital shaker overnight. Bacteria were collected and the plasmid isolated and purified using the Qiagen High Speed Plasmid Maxi Kit plasmid purification kit. Plasmid concentration and purity was determined spectrophotometrically by analyzing the absorbance at 260 and 280 nm.

#### **Culture of hMSCs and Transfection with Wnt5a Plasmid**

Human mesenchymal stem cells (hMSCs, Cambrex Corporation, East Rutherford, NJ or Lonza, Basel, Switzerland) were cultured in round 100mm plates using standard protocols and hMSCs media recommended by the supplier. When the cells had reached 60-90% confluence, they were harvested by trypsinization using trypsin kits from the cell supplier. The cells from one plate (approximately  $10^6$  hMSCs) were resuspended in 200µl hMSC nucleofactor solution (Amaya Biosystems, Gaithersburg, MD) with 4µg Wnt5a plasmid. The cells were split among two electroporation cuvettes and electroporated using program U-23 on an Amaya Nucleofector I. Transfected hMSCs (Wnt5a-hMSCs) were immediately resuspended in hMSC media and transferred to Costar Transwell permeable support inserts in 1.5ml hMSC media with 2.5ml hMSC media in the compartment below the insert. Since the transfection procedure resulted in 25% cell survival, two cuvettes of transfected cells were pooled and then split among three supports (1/3 of a 100mm plate per insert). Non-transfected control hMSCs were also transferred to Transwell inserts, but only 1/12<sup>th</sup> of a plate of nontransfected cells were placed in each support, since nearly 100% survival could be expected with the control cells.

#### **Confirmation of Wnt5a Expression**

An ELISA was performed on lysates from transfected Wnt5a-hMSCs and non-transfected control hMSCs plated in 100mm culture plates. Anti-mouse Wnt5a antibodies (R&D Systems, Minneapolis, MN) were used for capture and detection of Wnt5a in the cell lysates. The detection antibodies was biotinylated. Incubation with streptavidin-conjugated horseradish peroxidase (HRP) followed by development with a

colorimetric substrate was used for quantitation of the results. Plates were analyzed on a POLARstar Optima microplate reader (BMG Labtech, Durham, NC).

### **Isolation and Culture of Adult Canine Cardiomyocytes**

Canine cardiomyocytes were isolated from adult mongrel dogs of either sex according to published protocols.<sup>32</sup> Dogs were euthanized by an intravenous injection of pentobarbitone (80 mg/kg body weight), a left thoracotomy was performed, and the heart was quickly removed. Cardiomyocytes were isolated using a modified Langendorf procedure in which a wedge of left ventricle was perfused via a coronary artery with a  $\text{Ca}^{2+}$ -free solution containing collagenase and protease. The tissue was then minced, dispersed, and filtered to produce a single cell suspension.

### **Establishment of Co-cultures**

Isolated cardiomyocytes were transferred to laminin-coated 6-well plates in a  $\text{Ca}^{2+}$ -free buffer containing 1 un/ml insulin (Sigma, St. Louis, MO) at an overconfluent density and placed in a 37°C incubator for one hour. The media was gradually changed to  $\text{DMEM}^+$  media (high glucose DMEM [Invitrogen] supplemented with 5% fetal bovine serum [FBS, Invitrogen] and 1% penicillin/streptomycin [Invitrogen]) in increments of 12-15% at 15-60 minute intervals to slowly raise the  $\text{Ca}^{2+}$  concentration.

Cardiomyocytes were finally changed to 100%  $\text{DMEM}^+$ , with 2.5ml in each well.

The Wnt5a-hMSC or hMSC control cells in Transwell inserts (see above) were washed once with  $\text{DMEM}^+$  media before transfer of 2.5ml  $\text{DMEM}^+$  below the insert and 1.5ml above the insert and returned to the incubator for at least 1 hour. Inserts were then transferred to wells containing cardiomyocytes. In some experiments,  $\text{DMEM}^+$  supplemented with 100ng/ml insulin-like growth factor-1 (IGF-1; Sigma) was used in the final media addition for Wnt5a-hMSCs, hMSCs, and cardiomyocytes.

### **Quantification of Colony Formation in Co-cultures of Cardiomyocytes and Wnt5a-hMSCs**

Cardiomyocyte colonies were defined as clusters of 4 or more cardiomyocytes in close association. Using the 10× objective on an Olympus CK40 inverted microscope, a single vertical diameter of the area underneath an insert was scanned visually, and colonies were counted by hand. Diameters from three wells were counted for each group.

### **Immunohistochemical and Immunofluorescent Staining**

Colonies were removed from the plate by gentle trypsinization and replated onto CC2-treated chamber slides (Nunc, Rochester, NY) overnight. They were then washed briefly with phosphate-buffered saline (PBS), fixed for 15 minutes in 4% paraformaldehyde, permeabilized for 10 minutes with 0.2% Triton X-100, and washed twice with PBS.

Slides were stained with a primary antibody against Ki67 (Dako, Denmark) or sarcomeric  $\alpha$ -actinin (Sigma). For Ki67, epitope retrieval was performed by incubating in 95°C citrate buffer for 20 minutes prior to incubation with primary antibody. A biotinylated secondary antibody (Vector Laboratories, Berlingame, CA), followed by incubation with a streptavidin-conjugated HRP and development with a 3,3'-diaminobenzidine kit (Vector Laboratories) was used for detection. For sarcomeric  $\alpha$ -actinin, a secondary antibody conjugated to AlexaFluor488 (Invitrogen) was used for detection, followed by fluorescent imaging.

### **Anti-Fibroblast Surface Protein Antibody and Complement Treatment**

For experiments in which anti-fibroblast surface protein antibody ( $\alpha$ -FSP) was used in the cultures, cardiomyocytes were incubated for 40 minutes at room temperature in  $\text{Ca}^{2+}$ -free media with 1:200  $\alpha$ -FSP (Sigma). Cells were then incubated 45 minutes with 1:10 rabbit complement (Sigma). Cardiomyocytes were washed with  $\text{Ca}^{2+}$ -free medium and plated at a superconfluent density in 6-well plates. Post-plating protocols to raise the  $\text{Ca}^{2+}$  concentration and establish co-cultures were carried out as described above.

### **Time-Lapse Microscopy of Cardiomyocyte Co-cultures**

Ten to fifteen days after initiation of co-culture of cardiomyocytes with Wnt5a-hMSCs in Transwell plates, the culture vessels were transferred to a microscope-mounted humidified weather station for time-lapse imaging. A constant flow of 5%  $\text{CO}_2$  into the weather station was maintained.

### **Statistics**

Values given represent the mean  $\pm$  SEM. Results of Wnt5a expression levels were compared using a t-test. Colony numbers were analyzed using a Mann-Whitney Rank Sum test. Significance was accepted at  $p < 0.05$ .

### 3.1.3 Results

#### ***Wnt5a Expression in hMSCs***

Expression of Wnt5a in transfected human mesenchymal stem cells transfected with the Wnt5a plasmid was confirmed via an ELISA (Figure 1). Comparison of cell lysates from plain hMSCs and hMSCs transfected with Wnt5a showed  $5.723 \pm 0.046$  pg/ml Wnt5a in the Wnt5a-hMSC lysate vs.  $0.049 \pm 0.007$  pg/ml in the hMSC lysate ( $p < 0.001$ ).

#### ***Effect of Wnt5a and IGF-1 on Colony Formation in Cardiomyocyte Cultures***

Previous work from our laboratory indicated that co-culture of isolated canine cardiac myocytes with hMSCs<sup>30</sup> and Wnt5a-overexpressing hMSCs<sup>33</sup> could induce proliferation of the cardiac myocytes. Initial experiments adding Insulin-like Growth Factor 1 (IGF-1) to the cultures demonstrated qualitatively that Wnt5a-hMSCs with media supplemented with IGF-1 could further augment the rate of cardiomyocyte proliferation *in vitro* (data not shown). This proliferation resulted in the formation of what appeared to be colonies of dividing cardiac myocytes (Figure 2A). Quantification of these colonies demonstrated a dramatic increase in the number of colonies formed when cardiac myocytes were supplemented with IGF-1 and co-cultured with Wnt5a-hMSCs versus co-culture with plain hMSCs (Figure 2B). For purposes of quantification, colonies are defined throughout this chapter as four or more cardiac myocytes in tight association with one another.

Prior to colony formation, the cardiac myocytes were observed to lose their characteristic striated rod shape and become more spherical (Figure 3A). Many of these cells began to send out branching processes after a few days in culture (Figure 3B). By 10-14 days in culture, colonies of round myocytes could be observed. Staining of some of these colonies for Ki67, a nuclear marker for cells progressing through the cell cycle, indicated that these myocytes were in the cell cycle (Figure 3C). Staining of similar colonies confirmed that these cells also contained the myocyte marker sarcomeric  $\alpha$ -actinin (Figure 3D).

**Figure 1.** Expression of Wnt5a protein in hMSCs transfected with the Wnt5a plasmid. Protein levels determined by an ELISA on lysates from transfected (Wnt5a-hMSCs) and non-transfected (hMSCs) control cells. \*  $P < 0.001$ ; n=1 with 8 replicates for Wnt5a-hMSCs and 7 replicates for hMSCs.

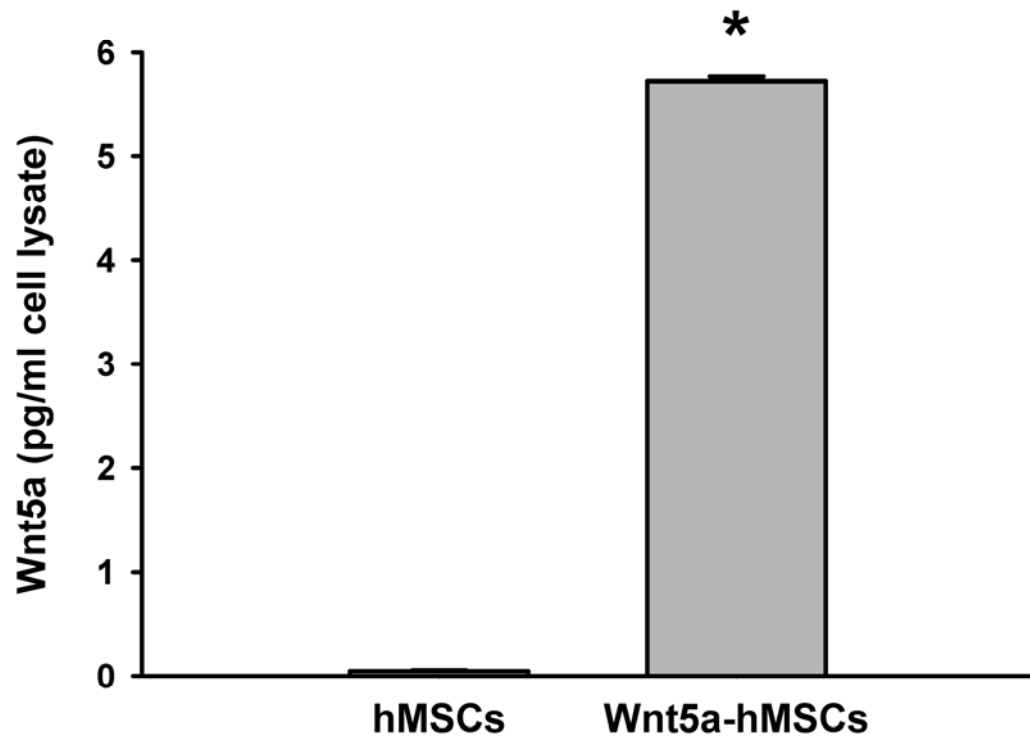


**Figure 2.** Colony formation in co-cultures of canine cardiac myocytes and hMSCs separated by a porous membrane. A) Colonies in the cardiomyocyte compartment imaged after 16 days in culture. B) Number of colonies formed in co-cultures with plain hMSCs (black bars) versus Wnt5a-hMSCs with IGF-1 in the culture media (gray bars) at 22-23 days in culture in four separate experiments. The colony numbers from each experiment were normalized to the hMSC colony numbers for the same experiment in order to calculate the normalized mean values (plotted against the right axis). \*  $P=0.029$  by Mann-Whitney Rank Sum analysis.

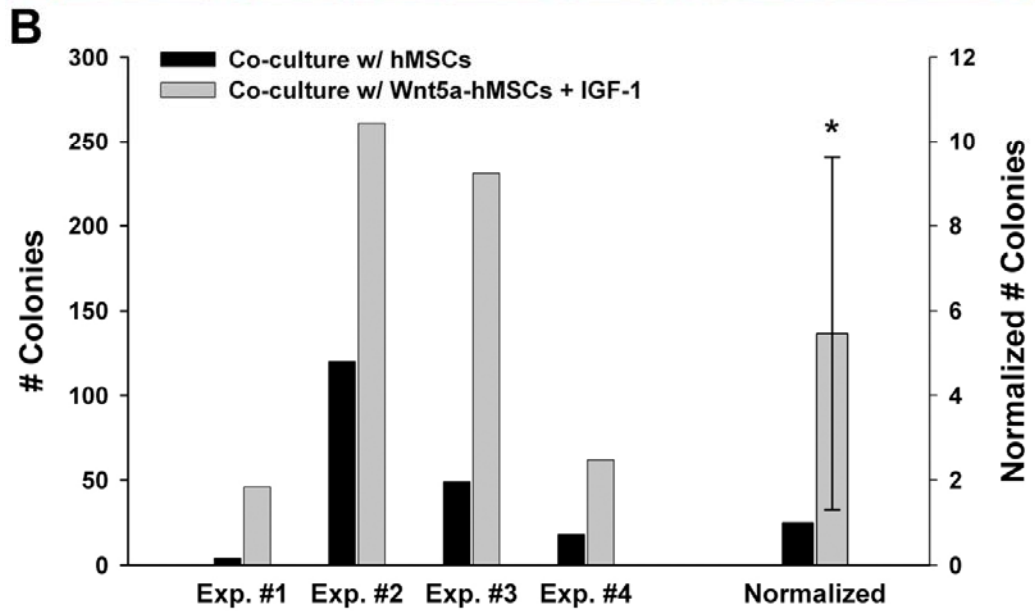
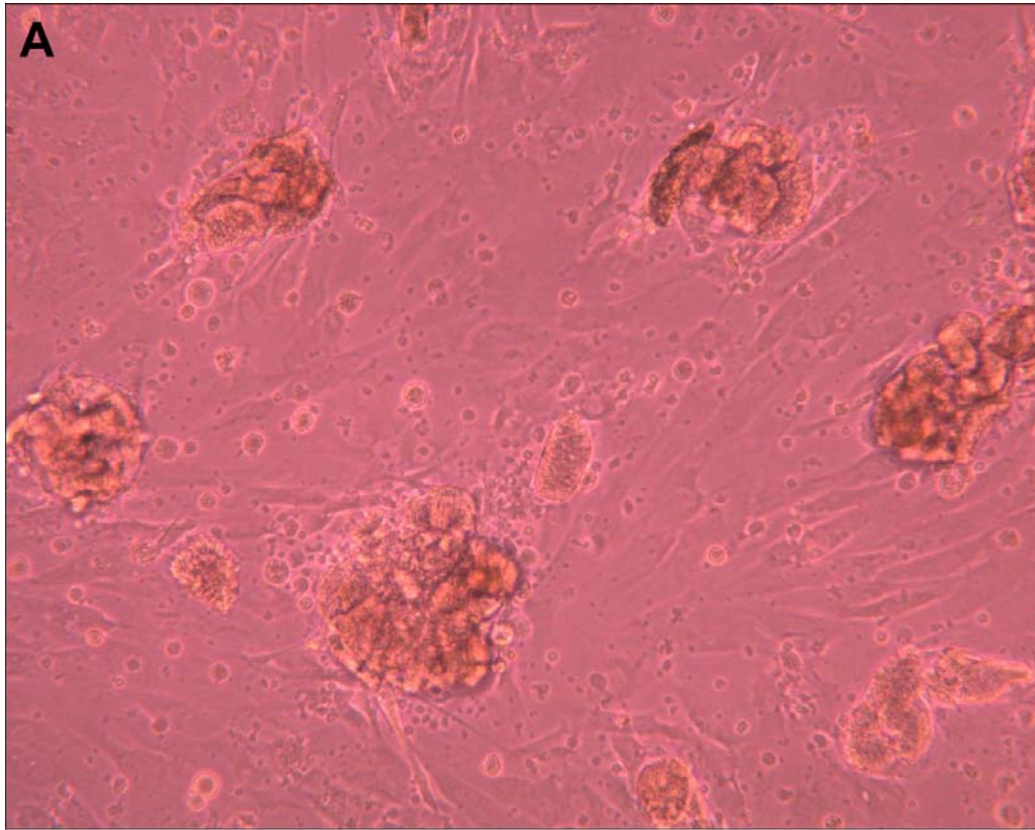
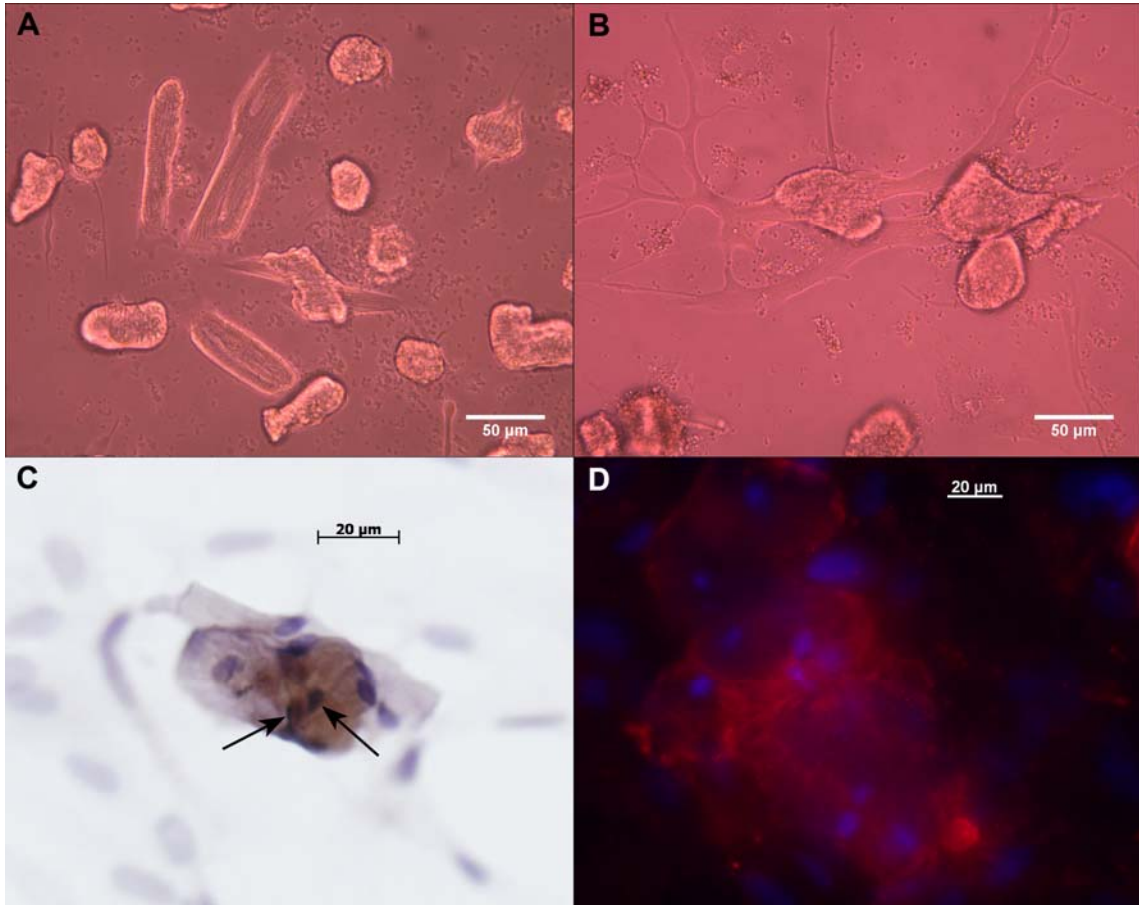




**Figure 3.** Morphological alterations and staining of cardiac myocytes in co-culture with Wnt5a-hMSCs. A) By three days in culture, the myocytes are at various stages of their morphological alteration to rounded cells. B) At 8 days in culture, many myocytes have grown branching processes. C) Staining for Ki67 (brown) at 30 days in culture demonstrates Ki67-positive nuclei in the colonies (arrows). D) Staining of similar colonies at 24 days in culture for sarcomeric  $\alpha$ -actinin (red) shows positive staining for this myocyte marker in the colonies. Blue = DAPI.



To determine whether the increase in colony numbers obtained with Wnt5a and IGF-1 could be attributed to one of these factors alone or the combination of the two, the effect of Wnt5a + IGF-1 was compared with Wnt5a-hMSC co-culture alone, hMSC co-culture supplemented with IGF-1, or hMSC co-culture without IGF-1 (Figure 4A&B). These results suggest that Wnt5a and IGF-1 work together to augment the rate of colony formation to a much greater extent than either factor alone.

In addition to the cardiac myocyte colonies, and number of additional large colonies could be observed in the cultures. These colonies were often larger, contained many smaller cells, and were spherical in shape (Figure 5). Based on the size of the cells in the colonies and the fact that they always appeared in areas of fibroblast overgrowth, it was presumed that these colonies were derived from fibroblasts in the cardiac myocyte cultures.

In an effort to address whether contaminating fibroblasts from the cardiac myocyte preparation may be the source of the Ki67<sup>+</sup> nuclei in cardiac myocyte colonies or otherwise contributing to cardiac myocyte colony formation, attempts were made to eliminate the fibroblasts from the cultures. Incubation of the myocyte preparation with an antibody to Fibroblast Surface Protein ( $\alpha$ -FSP) prior to plating, which prevented fibroblast attachment to the culture dish, resulted in a decrease in colony number in Wnt5a-hMSC + IGF-1 cultures to the level obtained with hMSC co-culture alone (Figure 6A). The number of colonies formed was also decreased by incubation with  $\alpha$ -FSP followed by incubation with rabbit complement, which binds to the  $\alpha$ -FSP antibody and actively kills the target cell (Figure 6A). In a second experiment, the effect of  $\alpha$ -FSP on Wnt5a-hMSC co-culture + IGF-1 was confirmed (Figure 6B). In this experiment,  $\alpha$ -FSP was also added to cardiac myocytes that were co-cultured with hMSCs, and colony formation was essentially eliminated at 14 days (Figure 6B).

### ***Time-Lapse Microscopy of Cardiomyocyte Division***

Several attempts were made to capture video images of cardiomyocytes undergoing mitosis in membrane-separated co-cultures with Wnt5a-hMSCs supplemented with IGF-1. Co-cultures of cardiomyocytes with Wnt5a + IGF-1 were kept in culture for 10-15 days to allow colony formation to begin prior to initiation of time-lapse imaging. In approximately 5 days-worth of video obtained from 5 time-lapse cultures, no example of cardiomyocyte division was observed. It must be noted, however, the difficulties in keeping the cells alive due to pH imbalances occurring in the time-lapse microscope incubator may have prevented the cells from undergoing cell division at the same rate that they would have in a better environment. Nevertheless, the complete absence of cell division suggests that the rate of cardiomyocyte proliferation may be lower than we had initially believed based on our colony count data.

**Figure 4.** Comparison of colony formation in Wnt5a-hMSC + IGF-1 co-cultures with Wnt5a-hMSC alone, hMSC + IGF-1, and hMSC co-culture alone. A) Line graph depicting the number of colonies formed in each of two experiments as a function of the number of days in culture. B) Number of colonies formed on culture day 15 in the same two experiments depicted in (A).

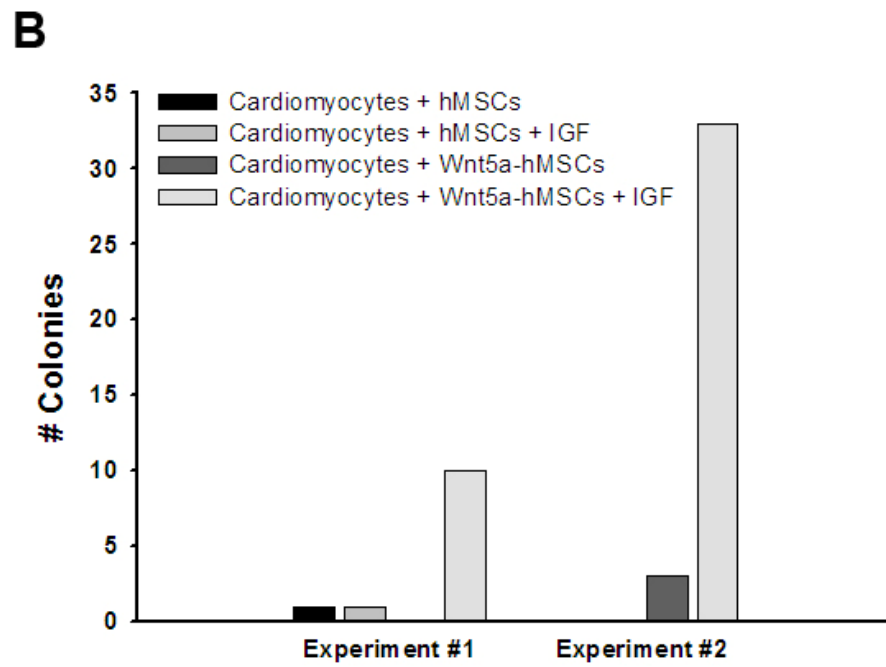
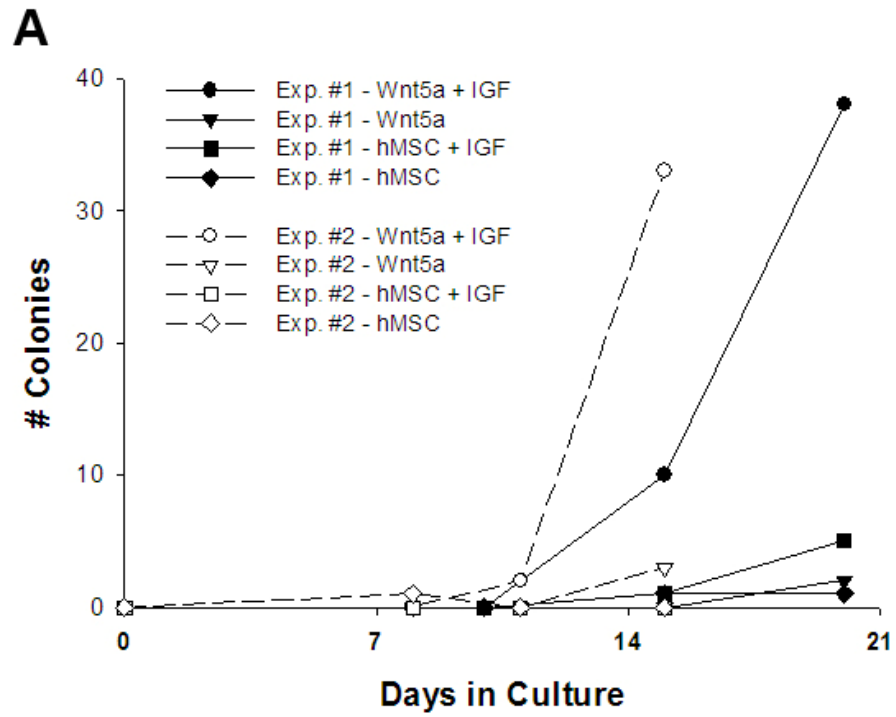


**Figure 5.** Large spherical colonies of fibroblast-like cells in a cardiac myocyte culture. The fibroblast colonies (arrows) can be distinguished from the cardiac myocyte colonies (arrowheads) by their large size, almost perfectly spherical shape, and the large number of small cells that comprise the colonies.

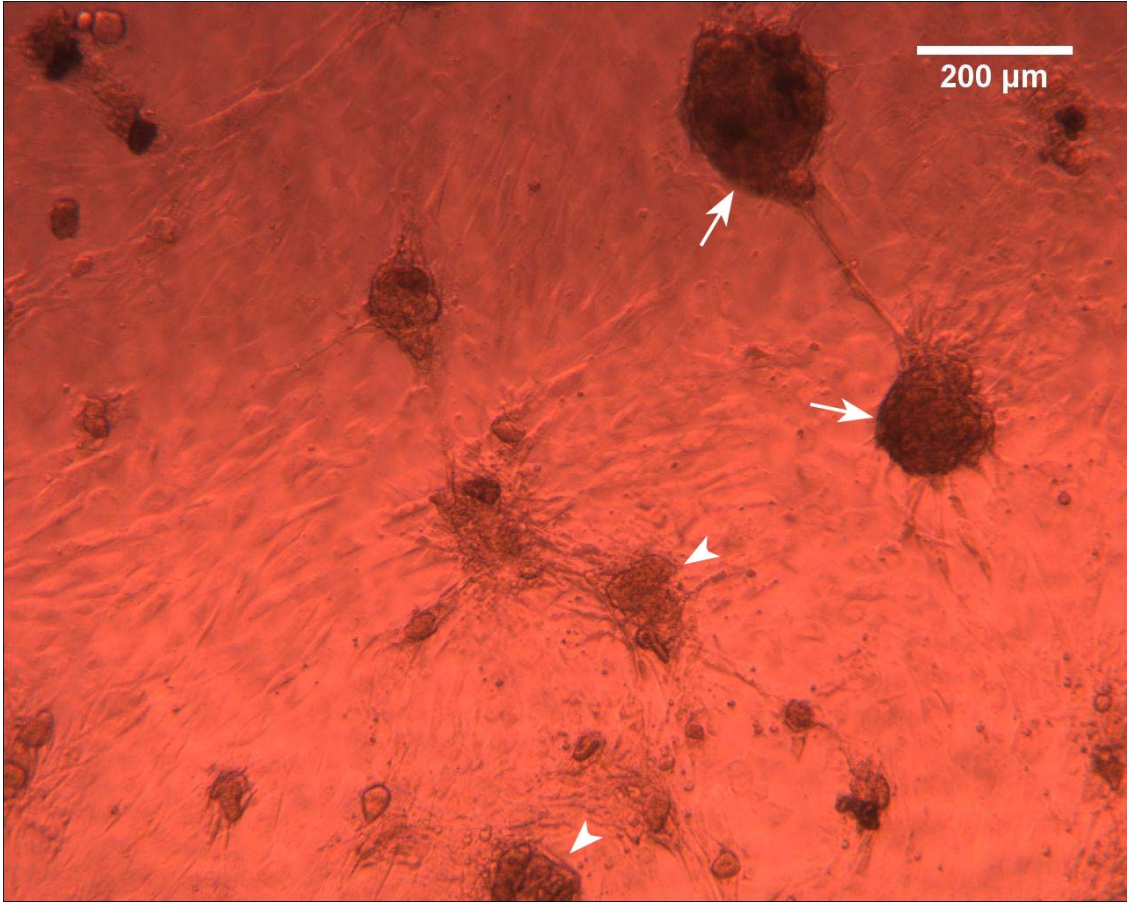
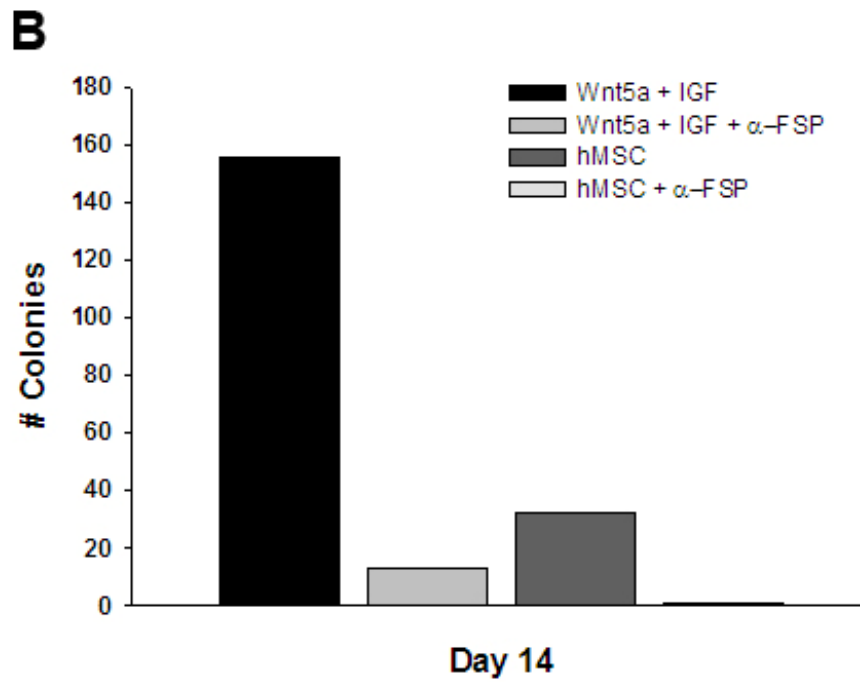
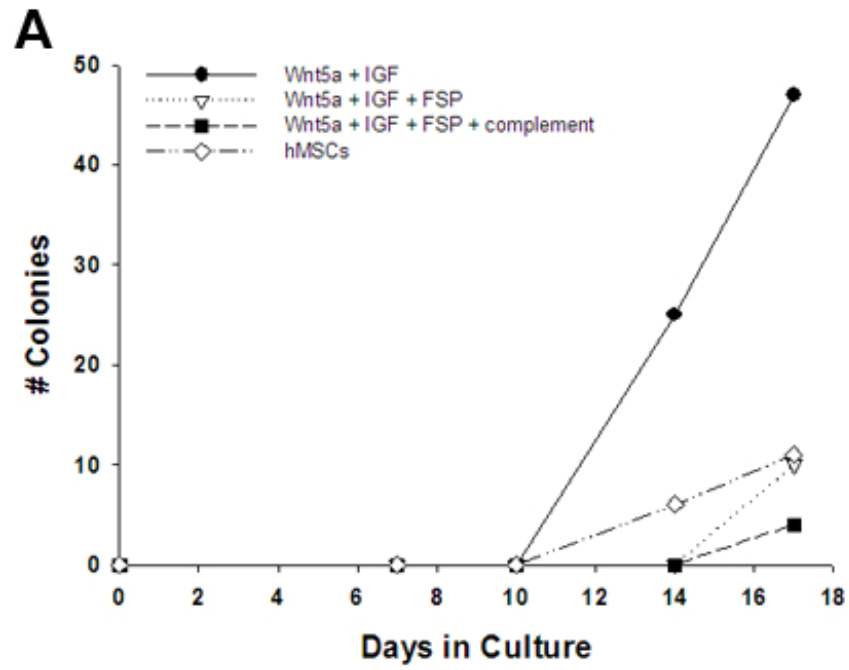


**Figure 6.** Number of cardiac myocyte colonies formed after incubation with  $\alpha$ -FSP antibody in each of two separate experiments. A) In the first experiment,  $\alpha$ -FSP or  $\alpha$ -FSP followed by complement was added to cardiac myocytes co-cultured with Wnt5a-hMSC and supplemented with IGF-1. The antibody to FSP decreased colony formation to levels seen with hMSC co-culture alone. B) The second experiment confirmed the result of (A) and showed that  $\alpha$ -FSP could virtually eliminate colony formation in hMSC co-cultures at 14 days.





### 3.1.4 Discussion

An ELISA assay confirmed expression of Wnt5a in transfected hMSCs. This plasmid had also been previously validated in our laboratory and was known to be effective. Co-culture of Wnt5a-hMSCs with adult canine cardiomyocytes produced a small increase in cardiomyocyte colony formation compared with plain hMSC co-cultures in one experiment and no increase in a second experiment (Figure 4). However, the addition of IGF-1 to the culture media in Wnt5a-hMSC co-cultures reproducibly resulted in a dramatic increase in cardiomyocyte colony formation compared with plain hMSC co-culture or co-culture with Wnt5a-hMSCs without IGF-1 (Figures 2, 4, and 6). To investigate whether this effect could be attributed solely to the IGF-1, two additional experiments were performed with IGF-1 and plain hMSCs compared with Wnt5a-hMSCs with and without IGF-1 and hMSCs without IGF-1. In neither of these experiments did IGF-1 produce an increase in cardiomyocyte colony formation compared with hMSCs alone (Figure 4). A large increase in colony formation was only seen in cultures with Wnt5a-hMSCs supplemented with IGF-1. These results strongly indicate that Wnt5a and IGF-1 work together to increase colony formation. In fact, this is consistent with the results from Fraidenraich et al.<sup>31</sup> suggesting that Wnt5a and IGF-1 together were responsible for stem cell-mediated rescue of cardiomyocyte proliferation in their thin-walled heart model of cardiac development.

However, our results do not allow us to rule out additional roles for other paracrine factors released by hMSCs. Since cell-cell contact between hMSCs and cardiomyocytes was prevented by the porous membrane keeping the hMSCs suspended one millimeter above the cardiomyocytes, we can be confident that any additional signals coming from the hMSCs were paracrine in nature, and not contact-dependent. Experiments were attempted in which purified Wnt5a and IGF-1 were added to culture media used to grow cardiomyocytes without hMSCs, but colony formation was not observed in these experiments (data not shown). This result is difficult to interpret since we could not confirm that the recombinant Wnt5a protein was active. Wnt proteins are dependent on palmitoylation for their activity,<sup>34</sup> and we cannot be sure whether the recombinant Wnt5a protein used was so activated or stable in powder form.

In an attempt to confirm that cardiomyocyte colonies were forming as a result of cardiomyocyte proliferation, colonies were stained for Ki67, a nuclear marker of proliferating cells (Figure 3C), and sarcomeric  $\alpha$ -actinin, a marker of myocytes (Figure 3D). Staining for Ki67 with a DAB detection kit showed positively stained nuclei in the colonies. Similar colonies showed evidence of sarcomeric  $\alpha$ -actinin, indicating that the cells were myocytes. The cells had lost their characteristic striated sarcomeric  $\alpha$ -actinin staining pattern, indicating that their sarcomeres had become disorganized or

completely disassembled. This is consistent with observations by others that proliferating cardiomyocytes dedifferentiate and lose their sarcomeric structure.<sup>35</sup> Despite exhaustive efforts, however, acceptable fluorescent labeling of Ki67 could not be achieved above the levels of autofluorescence of the cardiomyocytes. As a result, dual fluorescent staining could not be performed to allow for deconvolution of Z-stack images to confirm colocalization of Ki67 and sarcomeric  $\alpha$ -actinin.

Since primary cardiomyocyte cultures are invariably contaminated with fibroblasts which may explain the presence of Ki67<sup>+</sup> cells in the colonies, attempts were made to eliminate the fibroblasts from the cardiomyocyte preparations. This involved the use of an antibody against fibroblast surface protein ( $\alpha$ -FSP), which prevents the attachment of fibroblasts to culture vessels (Raymond Page, PhD, personal communication). Furthermore, by treating the cells with rabbit complement following incubation with the antibody, fibroblasts can be actively killed.<sup>36</sup> The use of  $\alpha$ -FSP or  $\alpha$ -FSP followed by complement prior to plating cells was highly effective in reducing fibroblasts from the cultures, though a small number of fibroblasts survived and proliferated. When the cardiomyocytes cultured with Wnt5a-hMSCs and IGF-1 were pretreated with  $\alpha$ -FSP, colony formation was severely diminished compared with the same culture conditions without  $\alpha$ -FSP (Figure 6A). Colony formation in hMSC co-cultures without IGF-1 was eliminated by pretreatment with  $\alpha$ -FSP (Figure 6B). There are at least two possible explanations for this observation. The first is that fibroblasts were participating in colony formation and may have even been contributing a significant amount of the cell mass to the colonies. The presence of multiple cells in the colonies which stain positive for cardiomyocyte markers, however, (Figure 3D) shows that fibroblasts could not account for the colonies in their entirety. Another explanation might be that cardiomyocytes are dependent on the fibroblasts to provide a “feeder” layer in order to proliferate, similar to embryonic stem cells. In any case, the possibility that the Ki67<sup>+</sup> nuclei in the colonies represented fibroblasts proliferating cannot be ruled out.

In an effort to obtain more definitive evidence of cardiomyocyte mitoses, time-lapse microscopy on co-cultures with Wnt5a-hMSCs + IGF-1 was performed. The resulting images showed no examples of cardiomyocytes proliferating. However, it is important to note that the conditions in the microscope incubator were not ideal for cell growth, and most cells (including fibroblasts) died within 48 hours. This was presumably due to the fact that the pH of the media became elevated over time because of an inability to adequately control the level of CO<sub>2</sub> inside the incubator chamber. Therefore, the absence of mitoses may simply reflect suboptimal cell growth conditions. In the first several hours of time-lapse, however, some of the cardiomyocytes appeared to move around the plate slightly, apparently riding on the more mobile and rapidly

proliferating fibroblasts. This leaves open the distinct possibility that the colonies of cardiomyocytes formed by aggregation, with fibroblasts serving as the “glue,” rather than by proliferation.

In the end, we could only conclude that if cardiomyocyte proliferation was, in fact, increased by Wnt5a and IGF-1, the increased rate was still below the threshold that could be detected using the methods described above. It is worth noting, however, that the baseline estimates for the cardiomyocyte proliferation index are on the order of 2 cardiomyocytes per 100,000 at any given time.<sup>19</sup> Therefore, even a very significant increase in the proliferative rate of a cell population that very rarely divides may still produce a rate too low to be easily detected *in vitro*, given the finite lifespan of cells in culture. Thus, while the data presented here do not provide convincing evidence of increased proliferation, they also do not rule out such an increase. Indeed, there are published reports which support a role for IGF-1 in cardiomyocyte proliferation during development<sup>37</sup> and postnatally<sup>38, 39</sup> and for a combined effect of Wnt5a and IGF-1 in development.<sup>31</sup> Nevertheless, considering the billion or more myocytes that must be replaced in heart failure, further augmentation of the proliferative rate may be necessary before cardiomyocyte proliferation can represent a viable therapeutic option.

## 3.2 *Cardiospheres are derived from fibroblasts*

### 3.2.1 Introduction

[Introduction adapted from Schuldt et al., 2008.<sup>40</sup>]

In 1961, a population of skeletal muscle progenitor cells (a.k.a, satellite cells or myoblasts) residing in skeletal muscle tissue was described in the frog,<sup>41</sup> followed by its identification in humans five years later.<sup>42</sup> Based on the similarities between skeletal and cardiac muscle, as well as the notion that stem cells conditioned by a cardiac environment may be best equipped to differentiate along cardiac lineages, more recent attempts have been made to search for stem cells within the heart itself. The first evidence for cardiac progenitor cells residing in the heart came from the laboratory of Piero Anversa in 2003. They identified a population of  $\text{Lin}^- \text{c-kit}^+$  cells in the adult rat heart that could at least partially differentiate into cardiac myocytes, smooth muscle cells, and endothelial cells both *in vitro* and *in vivo*.<sup>9</sup> These cells expressed cardiac proteins, including the cardiac transcription factor NKx2.5 and the contractile protein  $\alpha$ -sarcomeric actinin, and improved LV function in a myocardial infarction model in the rat.<sup>9,43</sup> Importantly, the differentiated myocytes isolated from the heart after injection contracted in response to electrical stimulation.<sup>9</sup> Following publication of these results, at least three additional populations of resident cardiac stem cells (CSCs) were described. These were identified by stem cell antigen-1 (Sca-1),<sup>44</sup> Hoechst exclusion (i.e., side population [SP] cells),<sup>45</sup> or the presence of the transcription factor isl1.<sup>46</sup> It is interesting to note that these different populations of stem cells do not overlap,<sup>12</sup> with the exception of the  $\text{Sca-1}^+$  and SP cardiac stem cells, and all are reported to have the ability to differentiate into cells with varying degrees of cardiomyocyte-like phenotypes.<sup>44-48</sup> The finding that a tissue long thought to have little potential for self-renewal would harbor multiple separate populations of stem cells was indeed unexpected.<sup>12</sup>

Although researchers have provided compelling evidence for the existence of resident cardiac stem cells, the fact is that these cells are somewhat rare ( $\sim 1 \text{ Lin}^- \text{c-kit}^+$  cell/ $10^4$  myocytes,<sup>9</sup> and 0.03% of total heart cells are SP cells<sup>44</sup>). Thus, their therapeutic potential may be limited by the difficulty of obtaining sufficient numbers of these cells from a patient's cardiac biopsy. Although the Anversa laboratory demonstrated vast proliferative potential in the  $\text{Lin}^- \text{c-kit}^+$  rat CSCs,<sup>9</sup> the number that can be obtained from a patient's cardiac biopsy and the amount of time required to expand them may be prohibitive. It is estimated that at least 1 billion cardiomyocytes are lost in heart failure.<sup>49</sup> As such, the requirements for expansion of these rare cell populations may be difficult to achieve. However, a method of rapidly expanding a more loosely defined population of CSCs from adult heart biopsies has recently been described. Messina et

al.<sup>28</sup> collected round “phase-bright” cells migrating out of small pieces of explant material from human and mouse myocardium and rapidly expanded them via growth in spherical structures termed “cardiospheres.” The mouse-derived cardiospheres, but not the human-derived ones, were reported to contract spontaneously in culture.<sup>28</sup> Cardiosphere-derived cells improved LV function after MI and showed Ca<sup>2+</sup> transients and spontaneous action potentials *in vitro* when co-cultured with neonatal rat ventricular myocytes.<sup>29</sup> Unfortunately, no indication of the total number or percentage of cells producing spontaneous action potentials was given.

While these results were encouraging, a number of questions have remained unanswered. Although neither group provides any explanation of the number of phase-bright cells they start with and the number of cardiosphere-derived cells (CDCs) produced, Smith et al.<sup>29</sup> does provide a graph of the number of population doublings of their cells over time starting at the day of cell harvest from the explants. Since they report that they injected  $5 \times 10^5$  cells (after 50 days in culture) into the infarct regions of mice with surgically-induced MIs, we can conservatively assume that they produced at least that many cells from a single 21mg biopsy specimen. Their data shows that the cells underwent an average of 5-6 population doublings over the course of 50 days in culture.<sup>29</sup> Therefore, to produce  $5 \times 10^5$  cells after 6 doublings, they would have had to start with 781 phase bright cells. Using the estimates of  $2 \times 10^7$  cardiomyocytes per gram of cardiac tissue<sup>1</sup> and one cardiac stem cell per  $10^4$  myocytes,<sup>9</sup> we would expect a 21mg biopsy to contain only 42 cardiac stem cells. Since the authors of these two studies suggest that the cardiospheres are enriched for cardiac stem cells (Messina et al. goes so far as to claim that their cardiospheres are clonally-derived), these numbers do not add up, even using the most conservative estimates of their cell numbers. Considering that Messina et al. show data suggesting that they obtained approximately  $5 \times 10^7$  *cardiospheres* from each patient biopsy (and hence, many fold more cells) the numbers become far more alarming. Taken together, these numbers suggest that the cardiospheres must be comprised of more than just cardiac stem cells.

Furthermore, both reports describe the phase-bright cells as a population of cells that egress from the cardiac explants only after the formation of a monolayer of fibroblast-like cells, over which they migrate. However, neither study offered any evidence confirming this theory regarding the means by which these cells appeared. And while both of these studies provided evidence of cardiac differentiation of their CDCs, neither revealed the percentage of cells that actually took on a cardiac phenotype.

During our investigations into cardiomyocyte proliferation (see above), in which primary cardiomyocytes were grown in culture, large spherical colonies of cells frequently formed in areas that were overgrown by contaminating fibroblasts. Since

these colonies were always presumed to be derived from fibroblasts, they were initially considered to be of little significance. However, their resemblance to the cardiospheres described by the Giacomello and Marban groups was very intriguing. The implications of cardiospheres actually being derived from fibroblasts were obvious: if cardiospheres are simply clusters of fibroblasts without any plastic potential, such information would be critical in informing future decisions regarding clinical trials with these cells. On the other hand, if cardiospheres represented fibroblasts which had adopted stem cell-like properties, such a finding would be even more important for its therapeutic potential. Therefore, we decided to pursue this observation further, giving rise to our hypothesis that cardiospheres were primarily derived from fibroblasts that had developed plastic potential.

### **3.2.2 Methods**

#### **Preparation of Explants**

Explant cultures were prepared as described by Smith et al.<sup>29</sup> and Messina et al.,<sup>28</sup> with the modifications described below. Adult mongrel dogs or Sinclair mini-pigs were euthanized by an intravenous injection of pentobarbitone (80 mg/kg body weight), a left thoracotomy was performed, and the heart and aorta were quickly removed. A piece of dermis was obtained from the thoracotomy site. The brain was exposed and a small piece of brain tissue was obtained.

Pieces of left ventricular (LV) mid-myocardium, right ventricular (RV) endocardium, left atrium (LA), dermis, aorta, and brain were minced into approximately 1mm<sup>3</sup> explants. These explants were partially enzymatically digested (with the exception of brain) with two 5-minute incubations in "Solution 1" (135mM NaCl, 5.4mM KCl, 1.0mM MgCl<sub>2</sub>, 0.33mM NaH<sub>2</sub>PO<sub>4</sub>, 10mM HEPES, 10mM D-glucose, and 2mg/ml bovine serum albumin) containing 0.2% trypsin (Sigma) and 0.1% collagenase (Worthington Biochemical Corp., Lakewood, NJ) at 37°C. Tissue fragments were then washed 3 times in Solution 1 to remove enzymes and isolated cells. Media was gradually changed over to "complete explant media" (CEM; Iscove's Modified Dulbecco's Medium [IMDM] supplemented with 10% fetal calf serum, 100 U/mL penicillin G, 100 g/ml streptomycin, 2 mM L-glutamine) in increments of 25% at 30-90 minute intervals. Explants were plated in fibronectin-coated 60mm culture dishes in 2.3 ml CEM and placed in a 37°C incubator for 3 days to attach. For cardiac explants, 15-18 pieces were evenly distributed in each plate, while aortic and dermal plates received 6-9 and 4-8 explants, respectively. Approximately 20 brain explants were placed in a single plate. Media changes were performed every three days with 4ml of CEM, except for brain explants, which received 3ml of CEM.

### **Formation of Cardiospheres/Fibrospheres**

Cardiosphere forming cells (CFCs) and fibrosphere forming cells (FFCs) were harvested from the explant plates when the fibroblast monolayer growing out from the explants reached confluence or near confluence across the plate. Plates were washed with Versene (Invitrogen) for approximately 1 minute prior to treatment with 0.05% trypsin (Invitrogen) at 37°C for 2-5 minutes. Trypsin was stopped with an equal volume of CEM, and the plates were washed once more with CEM, adding the wash to the collected cells. Cells were centrifuged and resuspended in cardiosphere growth medium (CGM; 35% complete IMDM/65% Advanced DMEM/F-12 mix containing 2% B27, 10 ng/ml epidermal growth factor [EGF], 80 ng/ml basic fibroblast growth factor [bFGF], 4ng/ml cardiotrophin-1, 1 unit/ml thrombin, 100 U/mL penicillin G, 100 g/ml streptomycin, and 2 mM L-glutamine). The cells were plated in poly-D-lysine-coated 6-well plates (cells from one explant plate split among 6 wells). One half of the media was changed every two days.

### **Preparation of CDCs and FDCs**

Cardiosphere-derived cells (CDCs) and fibrosphere-derived cells (FDCs) were isolated from the spheres by trypsinization. Spheres were collected and transferred to 15ml conical tubes. The spheres were washed with Versene prior to trypsinization for 5 minutes at 37°C with periodic trituration. Isolated cells were centrifuged and resuspended in CEM.

### **Culture of Fibroblasts (Lonza)**

Normal human dermal fibroblasts (NHDFs) and normal human lung fibroblasts (NHLFs) were purchased as frozen stocks from Lonza (Basel, Switzerland). These cells were thawed and plated in 60mm plates or 6-well plates according to manufacturer recommendations in Fibroblast Media (FBM, Lonza) supplemented with the FGM-2 bullet kit (Lonza). The plates may or may not have been coated with fibronectin prior to cell plating. After cell attachment, media was changed to CEM in most experiments. In one experiment, the CEM was supplemented with 10 ng/ml epidermal growth factor (EGF), 10 ng/ml PDGF, 10 ng/ml TGF- $\beta$ , or all three of these growth factors plus 80 ng/ml basic fibroblast growth factor (bFGF).

### **Membrane-Separated Co-culture of Fibroblasts with Cardiac Explants**

Cardiac explants were prepared as described above and transferred to Transwell permeable support inserts with 3.0  $\mu\text{m}$  or 0.4  $\mu\text{m}$  pore sizes, approximately 20-24 explants per insert. Transwell plates received 2.5ml CEM media below the insert and 1.5ml CEM in the insert. The inserts were incubated for 4-24 hours to allow the cardiac explants to begin to condition the media.



NHDFs or NHLFs were plated in 6-well plates coated with fibronectin as described above. After cell attachment, media was removed and the Transwell inserts containing cardiac explants or empty inserts, along with their media, were transferred to the wells containing the human fibroblasts. The media was allowed to permeate through the insert membranes to the fibroblasts below, and then 2.5ml CEM was added to each insert. Media was changed every two days by aspirating ~2ml of the media below the insert, allowing the media from the top compartment to drain to the bottom, and adding 2ml fresh CEM to each insert.

### **Co-culture with Rat Neonatal Ventricular Myocytes**

Rat neonatal ventricular myocytes were isolated and cultured as described previously,<sup>50</sup> with minor modifications. Hearts were removed from 2-day old neonatal rats, chopped into small pieces and digested with 1mg/ml trypsin at 4°C overnight, followed by four 2-minute incubations with 1mg/ml collagenase. Isolated cells were strained and pre-plated twice in 10% serum culture medium (M199 media with 10% fetal bovine serum [FBS], 12µM L-glutamine, 1% B12/penicillin-streptomycin, 3.5 g/L glucose ) for 45 minutes in T175 flasks to remove fibroblasts.

PDMS rings with a 5mm inner diameter and 7mm outer diameter were placed in the centers of fibronectin-coated coverglasses in 6-well plates. NRVMs were plated outside of the PDMS rings at superconfluence and placed in the incubator for 24 hours. NRVMs were then washed with PBS to remove poorly attached cells, and fresh 10% culture medium was added. Immediately prior to plating of CDCs, FDCs, CFCs, or FFCs, the media on the NRVMs was changed to CEM.

CDCs, FDCs, CFCs, or FFCs were harvested as described above and resuspended in CEM media containing 5µl/ml CM-Dil (Invitrogen). Cells were incubated for 20 minutes in a 37°C water bath, washed three times for 5 minutes at 37°C in CEM, and resuspended in CEM media. The Dil-labeled cells were plated in the center of the PDMS rings with or without NRVMs outside and left in the incubator to attach for 1.5 to 3 hours. The PDMS rings were then removed to allow the cells to share media.

### **Adipogenic, Osteogenic, and Chondrogenic Differentiation**

CDCs, FDCs, CFCs, or FFCs were harvested as described above and resuspended in CEM media. For adipogenic and osteogenic differentiation, the cells were plated in 6-well, 12-well, or 24-well plates. Adipogenic and osteogenic induction was initiated using kits available from Lonza. For adipogenesis, three to five cycles of the following media changes were performed: 2-3 days of exposure to adipogenic induction medium followed by 2-3 days of exposure to maintenance medium. Osteogenic induction was carried by feeding the cells with osteogenic induction medium every 3-4 days for 2-3 weeks. Chondrogenic induction was performed by pelleting  $2.5 \times 10^5$  cells in

chondrogenic induction medium containing TGF- $\beta$ 3. Complete media changes were performed every 2-3 days for 3-4 weeks.

At the end of the induction protocols, the cells were rinsed with PBS and fixed with 10% formalin. Adipogenesis was assayed using Oil Red O staining. Osteogenesis was assayed by staining for calcium deposition using Alizarin Red staining. Chondrogenic pellets were embedded in cryogenic cutting medium, sectioned for histology, and glycosaminoglycans were stained for using Safranin O.

### **Immunofluorescent Staining**

Cells co-cultured with NRVMs were washed with PBS, fixed for 15 minutes in 4% paraformaldehyde, permeabilized with 0.2% Triton X-100 (Sigma), and washed three times for 5 minutes with PBS. To detect sarcomeric  $\alpha$ -actinin expression, coverglasses were blocked with 5% horse serum (Vector Laboratories) for 30-45 minutes followed by incubation for 30 minutes with primary mouse antibody against sarcomeric  $\alpha$ -actinin (Sigma) at 1:200. After washing three times for 5 minutes with PBS, samples were incubated with secondary goat anti-mouse antibody conjugated to an AlexaFluor 488 fluorophore (1:200) for 30 minutes. Samples were washed three times in PBS and mounted on glass slides using VectaShield HardSet mounting medium with DAPI (Vector Laboratories). Slides were imaged for Alexa488 and Dil using an inverted Zeiss Axiovert 200M deconvolution microscope with an AxioCam MRm CCD camera.

### **Time-Lapse Microscopy of Explant Cultures**

Explant culture plates were placed on an Axiovert 200M microscope fitted with a heated humidified incubator chamber when the cultures were 7 to 15 days old. The CO<sub>2</sub> level in the culture chamber was actively regulated to maintain it at 5%. Images were acquired using phase contrast microscopy and the 10 $\times$  objective.

### **Statistics**

The “lifespans” of the phase-bright stage of phase-bright cells imaged using time-lapse microscopy were analyzed by LogRank analysis.

### 3.2.3 Results

#### Origin of “Phase-Bright” Cells

Explants of canine left ventricular (LV) tissue were placed in fibronectin-coated 60mm tissue culture plates and cultured for several days. As described by Messina et al.<sup>28</sup> and Smith et al.,<sup>29</sup> phase-bright cells were observed to appear following the formation of a fibroblast monolayer on the culture plate around the explant (Figure 7). The previous investigators described these cells as stem cells migrating out of the explant tissue on top of the fibroblast monolayer. If this were the case, one would expect a higher concentration of phase-bright cells around the explant and fewer at farther distances from the explant as the cells spread out. However, it was observed that the phase-bright cells were evenly distributed in the culture plate wherever fibroblasts were present. Furthermore, they also appeared in areas of the plate where explants had previously detached and were removed from the culture plate, leaving behind an area populated only by fibroblasts (data not shown). This led to the hypothesis that the phase-bright cells were derived from the fibroblast monolayer itself.

To address this possibility, cardiac explant plates were imaged using a time-lapse microscopy system which allowed us to carefully control temperature and CO<sub>2</sub> levels and keep cells alive indefinitely. The resulting images unequivocally demonstrate countless phase-bright cells arising from the fibroblast monolayer, undergoing mitosis, and then returning to the monolayer (Figure 8). The time-course of this series of events was typically on the order of two hours or less for a given cell, although some cells remained in their phase-bright stage for 30 hours or more. Often these “long-lived” phase-bright cells would return to the monolayer without undergoing mitosis. The vast majority of the phase bright cells observed in the video images could either be verified to have arisen from the fibroblast monolayer and/or incorporated into it at the end of their phase-bright stage (although the beginning or end of the phase-bright stage of cells present at the beginning or end of the video, respectively, could not be ascertained, and some cells wandered off camera during imaging). These video images demonstrated a very dynamic and rapidly cycling population of phase-bright cells. In no instance did a phase-bright cell appear to migrate out of the explants across the monolayer, as surmised by Messina et al.<sup>28</sup> and Smith et al.<sup>29</sup> This imaging technique was repeated several times, including using tissue from various locations within the heart (left atrium, right ventricular mid-myocardium, right ventricular endocardium), and the same results were observed each time.

**Figure 7.** Phase-bright cells (arrowheads indicate some examples) from a canine LV mid-myocardium explant imaged on culture day 13. The silhouette of the explant is visible in the top left corner.

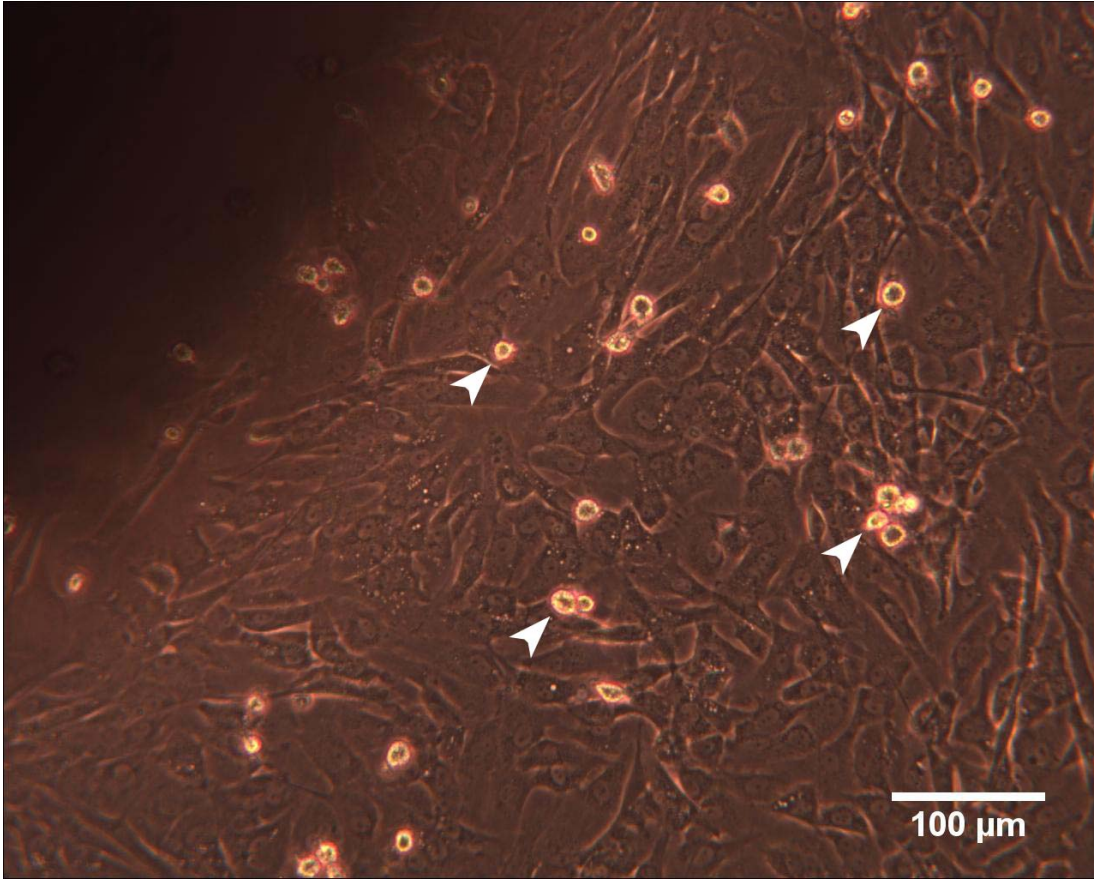
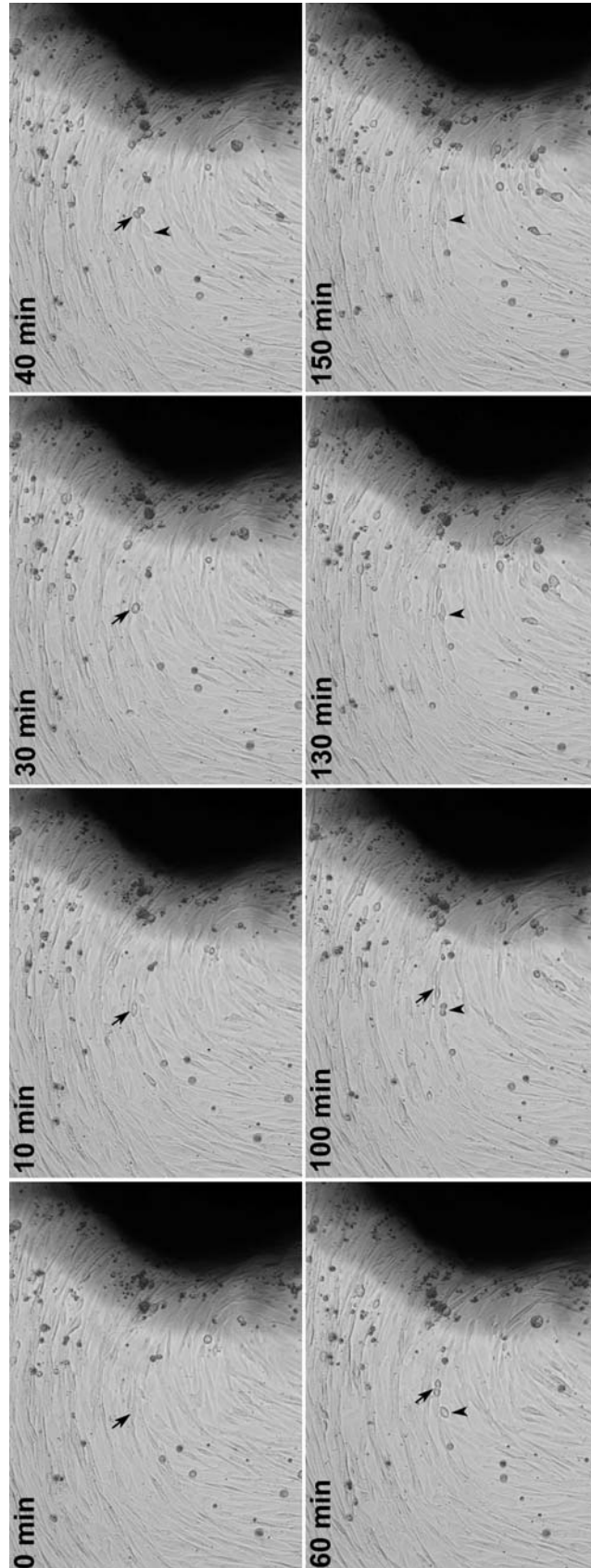


**Figure 8.** Time-lapse images from a canine left ventricular mid-myocardium explant culture. The arrows indicate a cell emerging from the fibroblast monolayer, becoming round and phase bright (30 min), undergoing mitosis (40 min), and finally returning to the fibroblast monolayer (100 min). Arrowheads indicate a second cell undergoing the same series of events (starting at 40 min). Countless examples of these events can be identified over time throughout the fibroblast monolayer.



### **Formation of “Cardiospheres”**

To confirm that the cells derived from these cardiac explants were capable of yielding “cardiospheres,” as described by Messina et al.<sup>28</sup> and Smith et al.,<sup>29</sup> the cells derived from canine right ventricular (cRV) endocardium explants were collected and replated in cardiosphere growth medium (CGM) on poly-D-lysine-coated plates as described by Smith et al.<sup>29</sup> with minor modifications as described in the Methods. The cells were imaged daily and observed for cardiosphere formation (Figure 9). At 4.5 hours after replating, the cells were attached to the plate and evenly distributed, displaying a morphology typical of fibroblasts. By 26 hours, the cells displayed a change in morphology, becoming more spindle-shaped and less flat. At 48 hours, the cells had begun to migrate toward one another, forming small clusters of cells with early spheres beginning to form in some clusters. At 72 hours, spheres were clearly evident in the plates with few cells remaining attached to the bottom of the plate. At 96 hours, some of the spheres had grown in size and even fewer cells remained attached to the bottom of the plate.

Since it remained possible that the spheres were formed by a population of phase-bright cells which are distinct from the fibroblasts but residing in the monolayer along with them, the phase-bright cells were washed off of the plate, collected, and replated in CGM media in one well of a 6-well poly-D-lysine-coated plate, while the fibroblast monolayer was collected separately and divided among the remaining five wells of the 6-well plate. The phase-bright cells washed off of the plate had not formed spheres after three days (Figure 10A). The fibroblasts, in the near absence of the phase-bright cells, formed spheres normally by three days (Figure 10B).

To investigate whether the cardiogenic growth factor cardiotrophin-1 (CT-1) was necessary for sphere formation, CGM media without CT-1 was used in the sphere formation protocol in some experiments. Fibroblasts collected from canine cardiac explant tissue formed spheres normally in the absence of CT-1 (data not shown).



**Figure 9.** Representative images showing the formation of spheres from cRV fibroblasts over time. At 4.5 hours, the cells are evenly distributed and appear typical of fibroblasts. By 26 hours after plating, the cells have become more spindle-shaped and less flat. At 48 hours, the cells have begun to migrate toward one another, forming clusters. By 72 hours, the clusters pull together into spheres. Relatively few fibroblasts remain attached to the plate, indicating that most have entered spheres. After 96 hours, the spheres are well-defined and growing in size. Scale bar = 200  $\mu\text{m}$  and applies to all images.

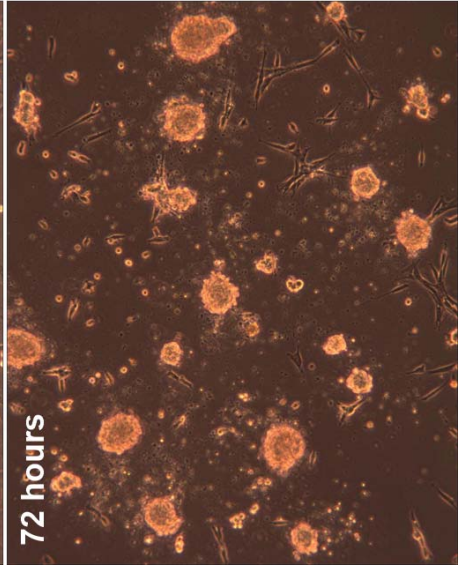
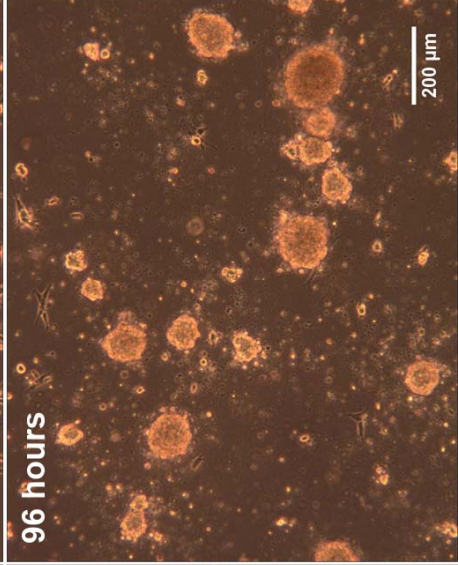
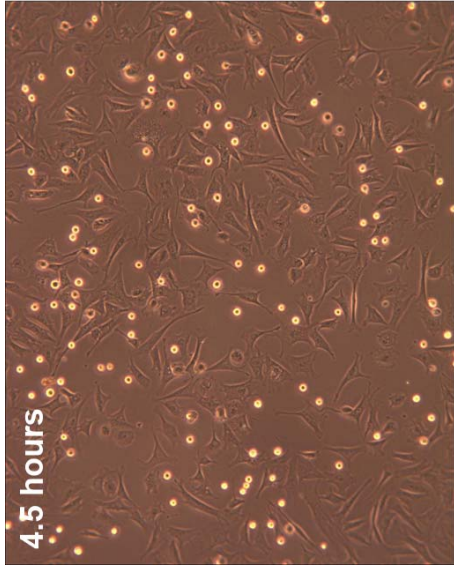
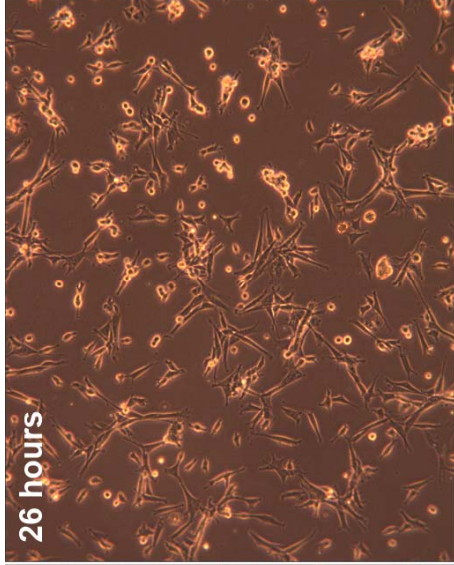
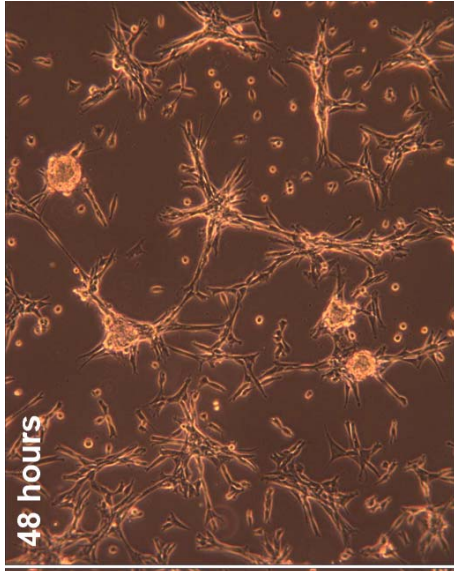
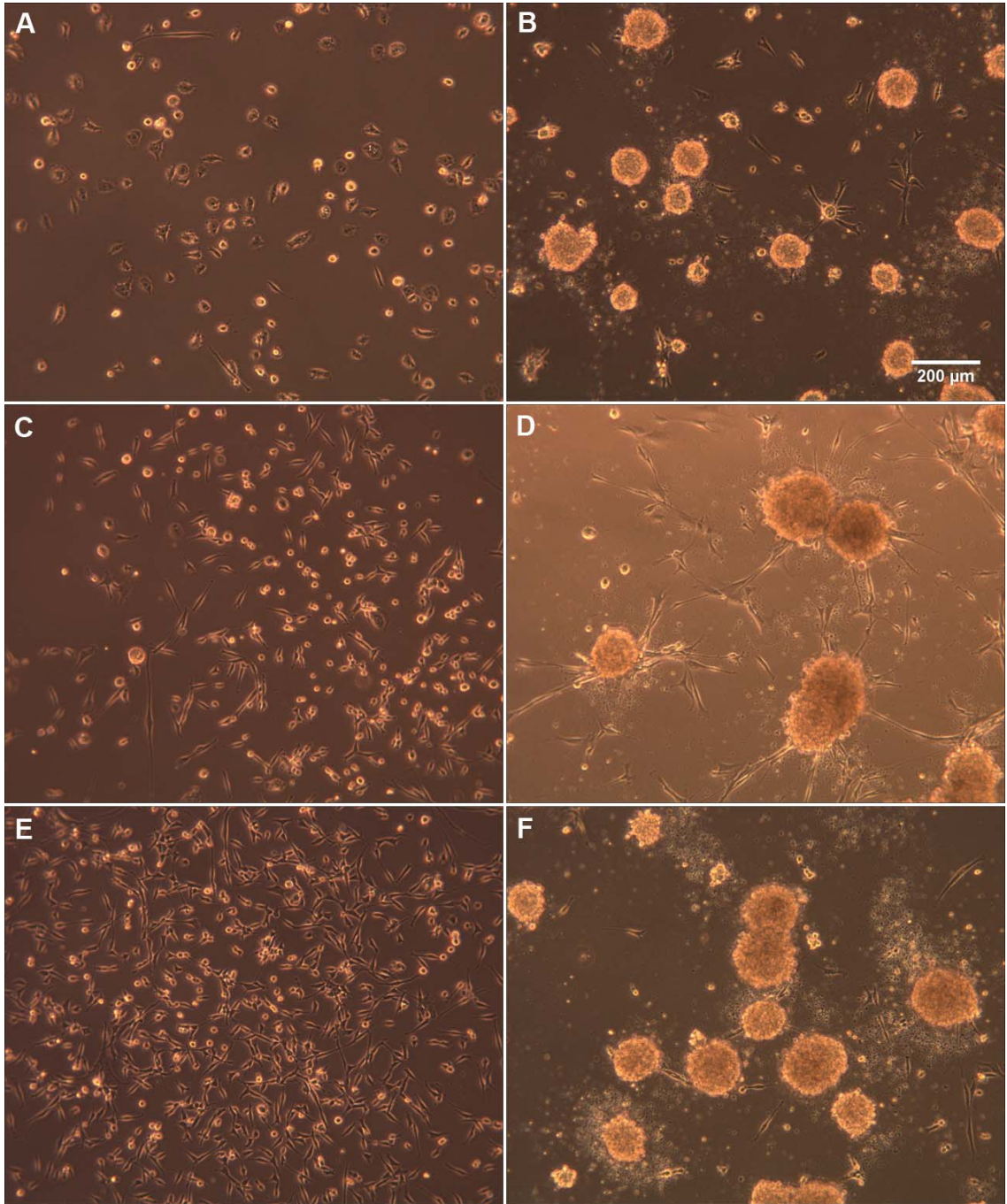


**Figure 10.** Sphere formation at day 3 using phase-bright cells washed off of the explant plate versus fibroblasts collected by trypsinization. A) The phase-bright cells washed off of a canine RV plate did not form spheres when replated in a single well together. B) The canine RV fibroblasts formed spheres normally in the near absence of phase-bright cells, which were washed off of the explant plate prior to trypsinization. C) Phase bright cells washed off of a canine dermal plate did not form spheres. D) Cells from the canine dermal fibroblast layer did form spheres in the absence of phase bright cells. E) Phase bright cells washed off of a canine aorta explant plate did not form spheres, while F) the fibroblasts from the aorta explant did in the absence of the phase bright cells. Scale bar = 200 $\mu$ m and applies to all images.



### **Phase-Bright Cells from Other Tissues**

Other groups have described the phase-bright cells collected from cardiac explants as cardiac stem cells.<sup>28,29</sup> Therefore, we wished to determine whether the formation of cardiospheres was, in fact, specific to cardiac-derived cells. To this end, other tissue sources were used to establish explant cultures and investigate the abilities of the obtained cells to produce spheres (henceforth referred to as “fibrospheres” when derived from any tissue other than cardiac).

#### ***Dermis***

Canine dermal explants were cultured under the same conditions as the cardiac explants. Several days after plating, a monolayer of fibroblasts formed. Phase bright cells appeared on the fibroblast monolayer, underwent mitosis, and returned to the monolayer (Figure 11). These fibroblasts were collected by trypsinization and replated in CGM media on poly-D-lysine-coated plates. The dermal fibroblasts underwent the same morphological changes and clustering that the cardiac cells did, and fibrospheres formed by day 3 (Figure 12).

As with the right ventricular explants, phase-bright cells washed off of the plate and transferred to a single poly-D-lysine-coated well in CGM media did not form spheres by day three (Figure 10C), while the fibroblasts collected by trypsinization after removal of the phase-bright cells did (Figure 10D).

#### ***Aorta***

Canine aortic explants cultured under conditions identical to those of the cardiac and dermal explants and imaged using time-lapse also displayed the emergence of phase bright cells from the fibroblast monolayer. These cells also underwent cell division and returned to the monolayer. Replating of the aortic fibroblasts produced fibrospheres in the same manner as the cardiac and dermal cells discussed above. Separate replating of the fibroblasts and phase-bright cells from the aortic explants resulted in sphere formation in the fibroblasts monolayer fraction (Figure 10F), but no spheres in the phase-bright cell fraction (Figure 10E).

**Figure 11.** Time-lapse images of a canine dermal explant culture. Arrowheads indicate cells which arise from the monolayer, becoming phase-bright. These cells then undergo mitosis and return to the fibroblast monolayer. Scale bar = 100 $\mu$ m.

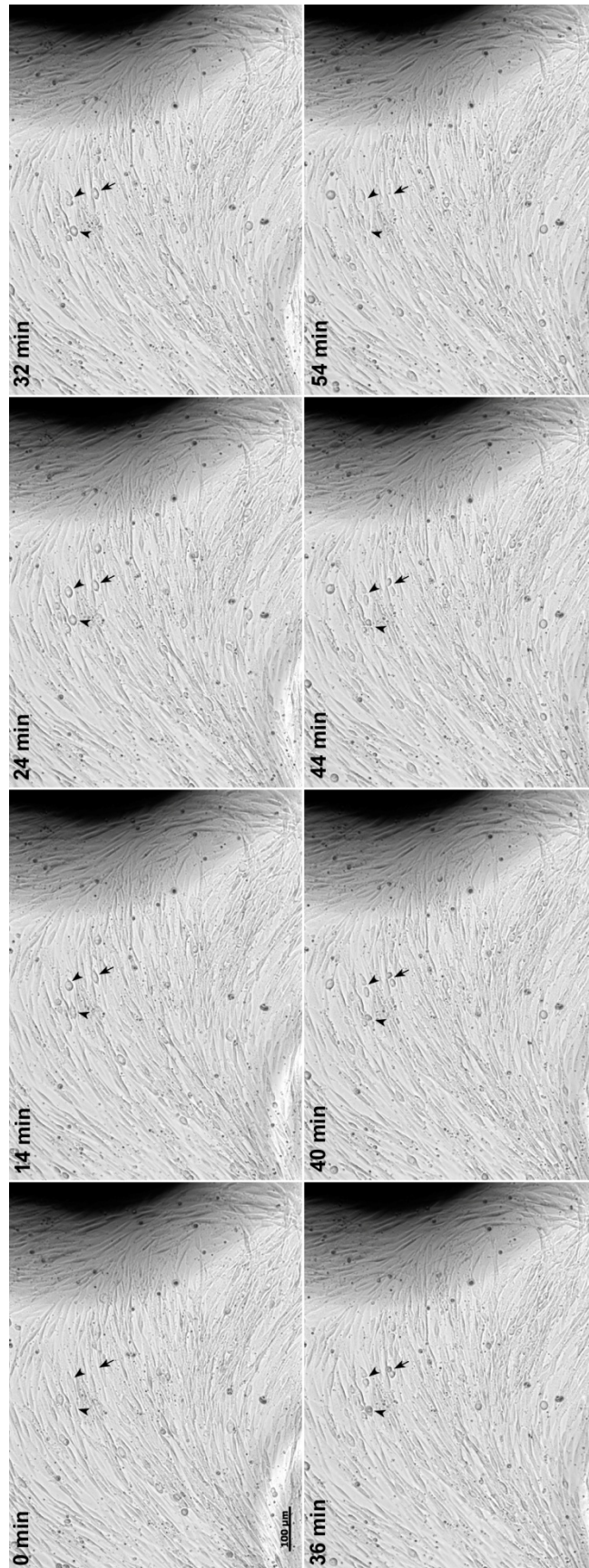
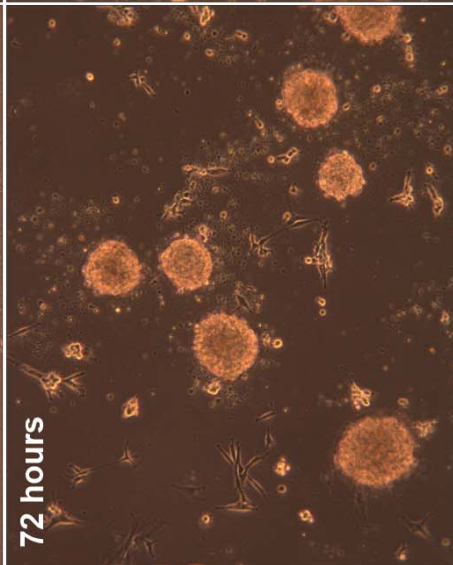
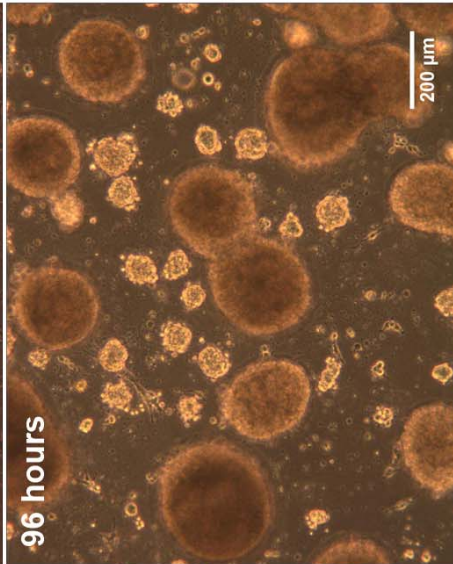
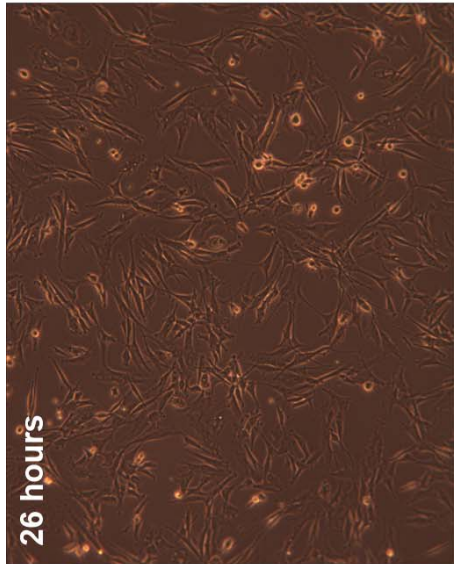
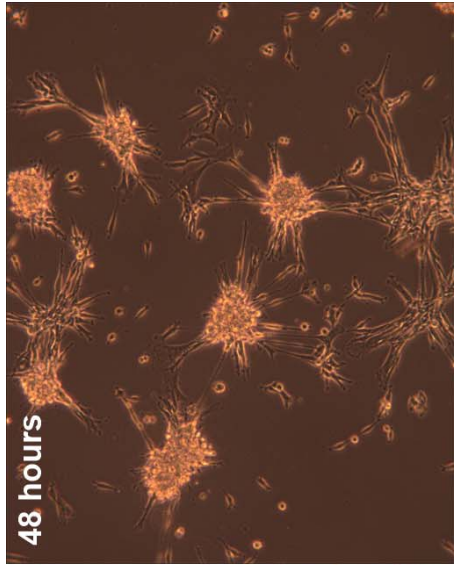


**Figure 12.** Fibrosphere formation from canine dermal-derived cells. The cells followed the same pattern of morphological changes and behaviors as the cardiac-derived cells. Scale bar = 200 $\mu$ m and applies to all images.





## **Brain**

As with the cardiac, dermal, and aortic explants, canine brain explants produced a monolayer of cells which resembled fibroblasts. From this monolayer, phase-bright cells appeared, underwent cell division, and then returned to the monolayer. Although spheres could be formed with these cells, they did not form spheres as efficiently as cardiac-, dermal-, or aortic-derived cells, with many cells remaining attached to the plates. In addition to the fibroblast-like cells, another population of cells with a more neural phenotype populated regions of the plates. Although these cells were never fully characterized, it is believed that they may be neurons, astroglia, or oligodendrocytes. Due to the mixed population of cells growing out from these explants, further experiments were not performed using brain tissue.

## **Porcine Tissue**

To ensure that the canine results are not species-specific, and to replicate our data using the same animal model as the Marban group,<sup>29</sup> we investigated the ability of tissues from the pig to form cardiospheres and fibrospheres. Explants from porcine right ventricular endocardium, dermis, and brain were cultured under the same conditions using the same media as described above for canine explants.

### ***Porcine Right Ventricular Endocardium***

As with the canine cardiac explants, porcine RV endocardium explants gave rise to a layer of fibroblasts around the explants upon which phase-bright cells appeared, divided, and returned to the monolayer (Figure 13). However, in the case of the porcine tissue, the time-course of monolayer formation was slower. While the canine RV explants produced a fully confluent monolayer spanning the plate within 7-10 days, the porcine tissue typically required 14 days or more to produce a confluent layer covering the entire plate. Consistent with this observation was the fact that the proliferation rate of the fibroblasts on time-lapse microscopy appeared to be much slower in the porcine explants. Furthermore, the population of “long lived phase-bright” cells was much more prominent in the porcine cultures. These cells appeared to persist in the phase-bright stage for many hours to even days, often without undergoing mitosis. However, a true sense of the average time in the phase-bright stage of these long-lived cells could not be ascertained due to the finite nature of the video (in both temporal and spatial terms) and the mobility of the cells.

Cells harvested from the porcine RV explants and replated in CGM media on poly-D-lysine coated plates also produced cardiospheres (Figure 14A). However, the porcine cardiospheres tended to take a day or two longer to form and were often

smaller in size compared to the canine cardiospheres. Phase-bright cells washed off of the plates prior to trypsinization did not yield spheres, while the trypsinized fibroblasts from the monolayer did.

### ***Porcine Dermis***

It typically took on the order of a month or more for a fully confluent monolayer to cover the plates of the porcine dermal explants. However, the canine dermal tissue produced a confluent monolayer in roughly half that time with a similar amount of explant tissue. This is consistent with the observation that 7.1 cells/hour became phase-bright in a single 0.565 mm<sup>2</sup> field of view in time-lapse images of the porcine dermal explants, while 9.9 cells/hour became phase-bright in the canine dermal explant plate in the same size field of view. This suggests an approximately 40% increased proliferation rate of the canine dermal cells compared to the porcine dermal cells.

“Survival curves” of the length of time cells remained in their phase bright stage were compared between canine and porcine dermal explants (Figure 15). Although the mean time in the phase bright stage was virtually identical in the two cultures (canine = 63 ± 6 minutes; porcine = 62 ± 17 minutes), the overall survival curves were significantly different ( $p < 0.001$  by LogRank analysis). This can be attributed to the typically shorter “lifespan” of most of the porcine phase-bright cells (median value = 36 minutes vs. 46 minutes for canine), and by the occurrence of two cells that remained phase-bright for exceptionally long times in the porcine culture (762 and 1624 minutes). In contrast, no canine cells remained phase bright more than 400 minutes.

Cells collected from the porcine dermal fibroblast monolayer also produced fibrospheres when replated on poly-D-lysine-coated plates in CGM. This process also took longer than in the canine dermal fibrospheres, with spheres typically beginning to form on day three or four. Porcine dermal fibrospheres were smaller in size than their canine counterparts (Figure 14B), but enlarged over time.

**Figure 13.** Time-lapse images of porcine RV explants. Arrowheads indicate individual phase-bright cells arising from the fibroblast monolayer, dividing, and returning to the monolayer. Scale bar = 100 $\mu$ m.

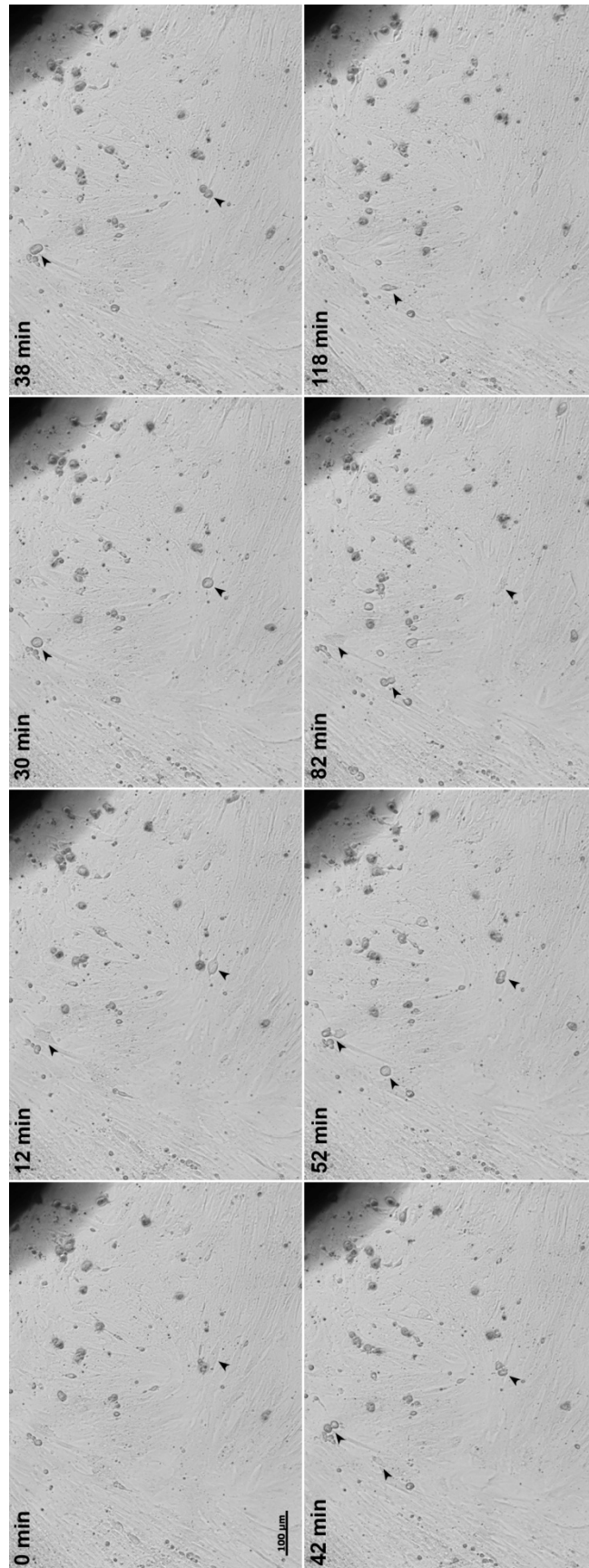


**Figure 14.** Cardiospheres and dermal fibrospheres derived from porcine tissue. A) Cardiospheres from porcine RV after 4 days of culture in CGM on poly-D-lysine-coated plates. B) Fibrospheres from porcine dermis after 4 days of culture in CGM on poly-D-lysine-coated plates. Note the smaller size of the porcine dermal fibrospheres compared to canine dermal fibrospheres (Fig. 12).

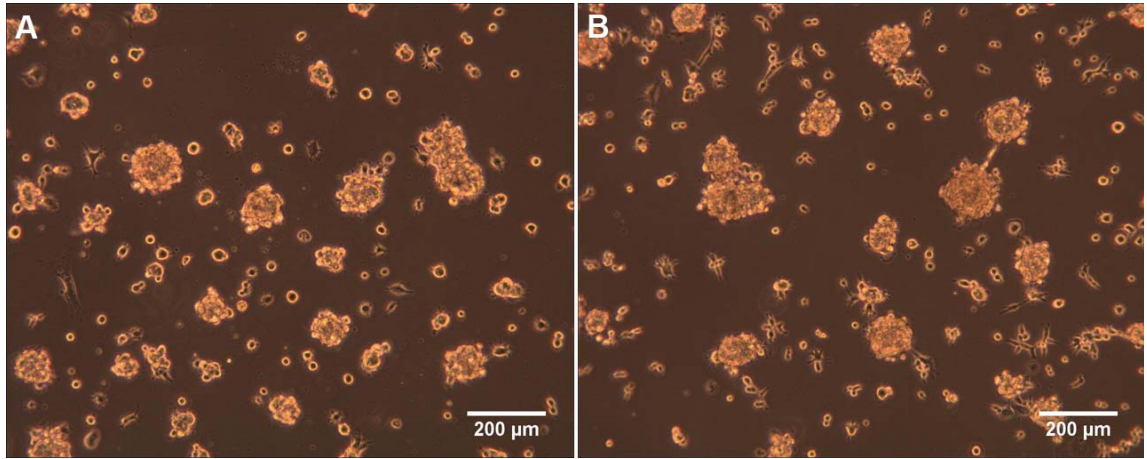
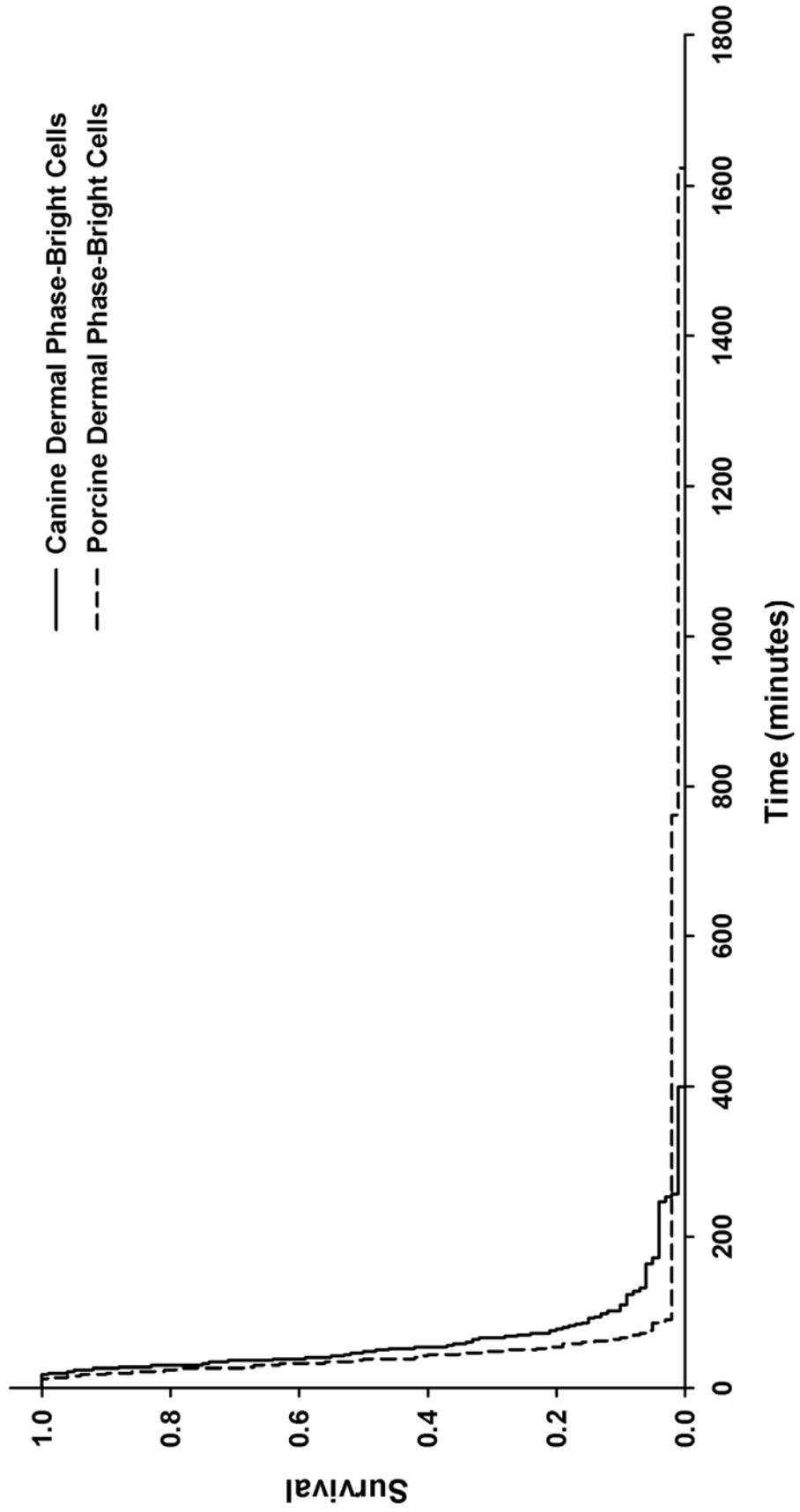


**Figure 15.** “Survival analysis” of canine versus porcine dermal phase-bright cells. The curves represent the time that 100 phase-bright cells in each group remained in the phase-bright stage before returning to the fibroblast monolayer. Although the median time spent as a phase-bright cell was shorter in the porcine cultures than the canine, the mean values were the same, due to the two cells that remained phase bright for over 700 minutes in the porcine culture.  $P < 0.001$  by LogRank analysis.



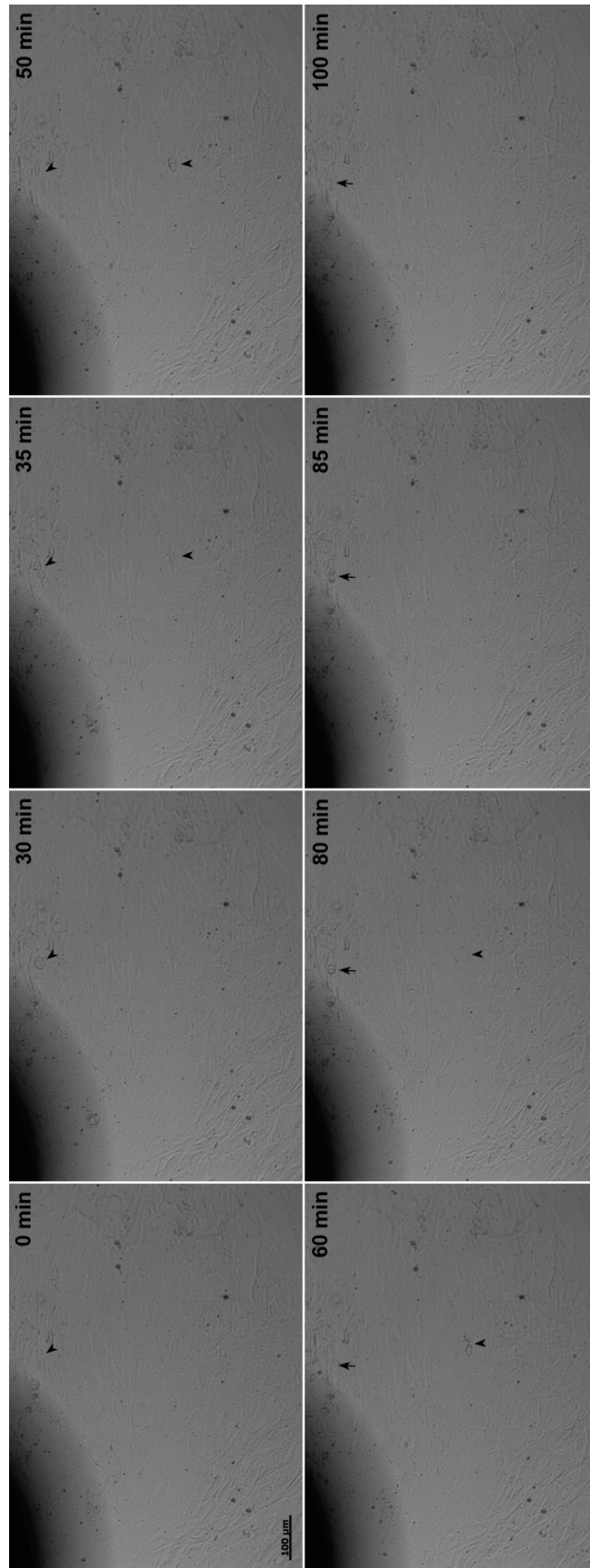


## **Human Fibroblasts**

Human right atrial appendage tissue was obtained from two patients undergoing cardiac surgery, and explants were prepared for culture as described above. The tissue obtained from these patients was very fibrotic, with little muscle tissue present. Explant cultures produced a monolayer of fibroblasts, although the layer was not as dense as that seen with canine or porcine tissue. Time-lapse microscopy revealed the appearance of phase-bright cells from the monolayer which underwent mitosis and returned to the monolayer (Figure 16). The appearance of these phase-bright cells was less frequent than in the canine or porcine cultures. The occurrence of cells remaining in the phase-bright stage for several hours was also lower than observed in the canine cultures and much lower than in the porcine cultures. Most of the long-lived phase-bright cells in the human cultures could be observed to either return to the monolayer or undergo apoptosis. The cells obtained from one of these cultures were replated in CGM media on poly-D-lysine-coated plates and did not form cardiospheres.

To test cells from other human sources, cryopreserved primary fibroblasts were purchased from Lonza (Basel, Switzerland). These included cells from three adult human tissue sources: normal human dermal fibroblasts (NHDFs), normal human lung fibroblasts (NHLFs), and aortic adventitial fibroblasts (AoAFs). Co-cultures were established in which NHDFs were cultured with explants from canine RV or LA separated by a porous membrane. Control cells were cultured alone. Co-culture of NHDFs with LA tissue resulted in fibrosphere formation when the NHDFs were re-plated under sphere-forming conditions. Likewise, NHLFs co-cultured with human RA tissue separated by a porous membrane produced fibrospheres. Control NHDFs and NHLFs that were cultured alone instead formed a confluent layer of cells in the poly-D-lysine-coated plates which subsequently lifted off of the plate as one large mass. It was later determined that some fibroblasts from the cardiac explants were able to pass through the 3 $\mu$ m pores in the membrane. Nevertheless, the majority of the cells in the lower compartments of the plates were most likely NHDFs or NHLFs for the following reason: these cells would be expected to proliferate at roughly the same rate as the control cells without cardiac explants. The fact that the control cells grew to confluence prior to harvest indicates that the cells co-cultured with cardiac tissue would have also grown to confluence independent of any contribution from canine cardiac explant cells.

**Figure 16.** Time-lapse images from a human RA explant culture. Phase-bright cells arise from the fibroblast monolayer, undergo mitosis, and return to the monolayer in the same fashion described for canine and porcine tissue. However, the frequency of phase-bright cell appearance was lower in the human RA explant cultures than the canine or porcine cardiac cultures. Scale bar = 100 $\mu$ m.



In some instances, NLHFs cultured alone produced a small number of spheres at the periphery of the poly-D-lysine plates from cells left behind after the large mass of cells detached (Figure 17A). A repeat of the experiment in which NHLFs were co-cultured with canine LA separated by a membrane with 0.4 $\mu$ m pores (which cells do not pass through) produced no spheres using the standard protocol. However, the cells did begin to undergo the morphological changes which precede sphere formation, in which they became more spindle-shaped and less flat and began to gather into clusters. However, due to cell proliferation preceding this change, the clusters were all interconnected. This resulted in a single large mass of cells detaching from the plate. Trituration of these cells at the stage of cluster formation resulted in many fibrospheres (Figure 17B).

NHDFs were also cultured under conditions recommended by Lonza in fibroblast media (containing basic fibroblast growth factor; bFGF) or alternatively in CEM supplemented with either transforming growth factor- $\beta$  (TGF- $\beta$ ), platelet-derived growth factor (PDGF), epidermal growth factor (EGF), or all four of these growth factors for 13 days in the absence of explant tissue to see if any of these growth factors or the combination of all four could activate the fibroblasts to form spheres. Upon replating these cells in separate poly-D-lysine coated plates in CGM media without CT, none of them formed spheres.

### **Differentiation of Sphere-Derived Cells**

To test the cardiogenicity of the cells derived from the spheres, a modification of the protocol used by the Marban group<sup>29</sup> to drive cardiac differentiation was employed. Cardiosphere-derived cells (CDCs) were co-cultured with rat neonatal ventricular myocytes (NRVMs) for 4 to 6 days. Likewise, fibrosphere-derived cells (FDCs) from dermal explants were tested for their ability to differentiate into cardiomyocytes. To further test the plastic potential of the CDCs and FDCs, adipogenic, chondrogenic, and osteogenic differentiation protocols were also employed.

#### ***Cardiac Differentiation of CDCs***

Canine CDCs co-cultured with rat NRVMs showed evidence of differentiation into cardiac myocytes with sarcomeric structure. Staining for sarcomeric  $\alpha$ -actinin demonstrated clear sarcomere formation in a small number of CDCs (Figure 18). It is estimated that 1 in 500 to 1 in 1000 cells showed evidence of cardiac differentiation in these cultures. The maturity of the sarcomeres (i.e., degree of organization) varied from highly organized striations to mostly disorganized sarcomeric  $\alpha$ -actinin staining. This differentiation was reproduced in six of six cultures of canine CDCs. Results from porcine CDCs were identical to those seen with canine cells.

**Figure 17.** Fibrosphere formation with NHLFs. A) NHLFs cultured alone produced a small number of fibrospheres at the periphery of the poly-D-lysine-coated wells from cells left behind after the large mass of cells detached from the plate. B) NHLFs grown in membrane-separated co-culture (0.4 $\mu$ m pores) with canine LA tissue formed fibrospheres when the cells were triturated after clusters began forming on the bottom of the poly-D-lysine-coated plate. Without trituration, the clusters became interconnected, resulting in a single large cell mass, rather than individual spheres. Scale bar applies to both images.

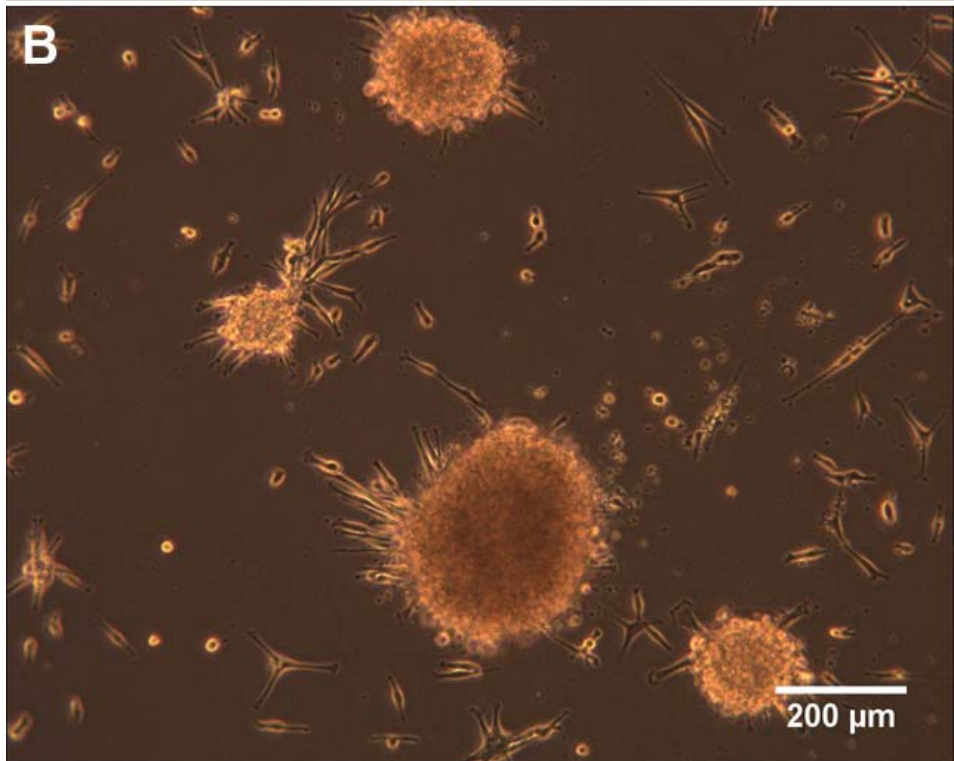
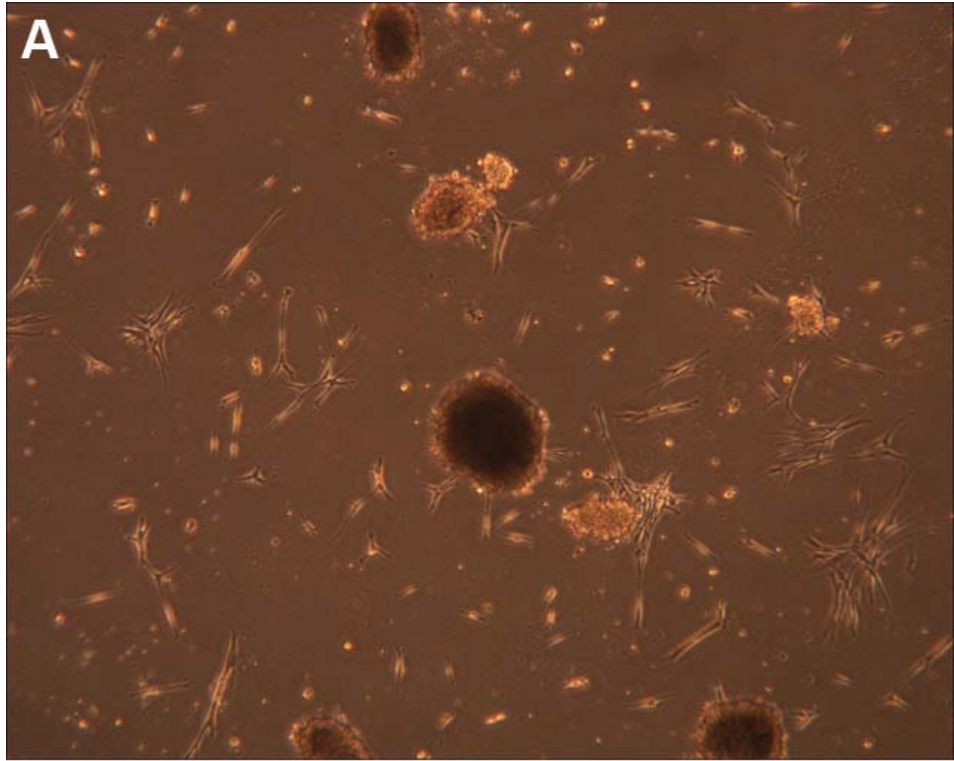
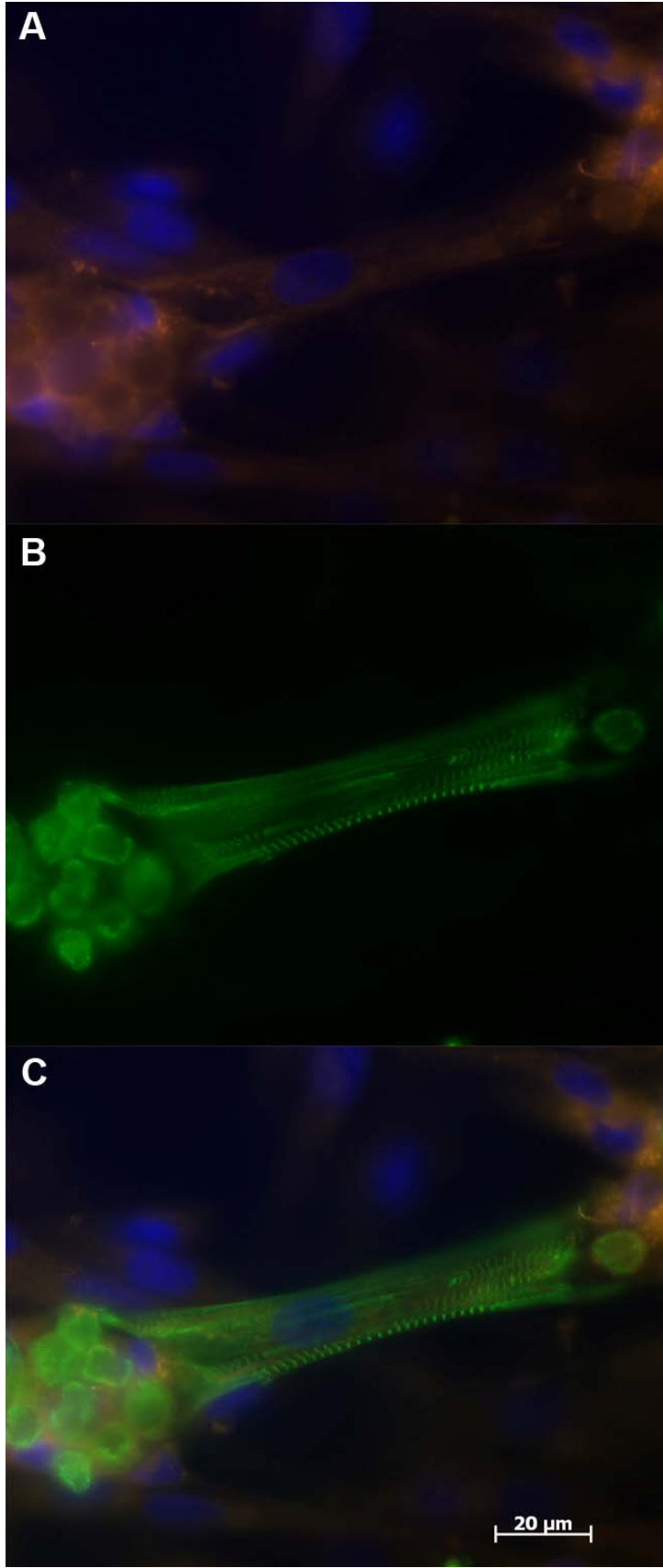


**Figure 18.** Cardiac differentiation of cardiosphere-derived cells. A) Dil label used to track CDCs. B) Sarcomeric  $\alpha$ -actinin staining. C) Merged image showing co-localization of the Dil and sarcomeric  $\alpha$ -actinin indicating cardiomyocyte differentiation of the CDC.





Images of NRVMs in the same cultures taken using the same microscope settings and exposure times demonstrated that these cells do not autofluoresce in the spectral range of the Dil label at levels sufficient to cause exposure in the short times used for imaging Dil (typically 35-100 msec). Furthermore, several instances of brightly Dil-labeled CDCs that had migrated into the area of NRVMs were observed, and in no instances did the surrounding NRVMs take up significant levels of Dil.

### ***Adipogenic Differentiation of CDCs***

Neither CDCs derived from canine nor porcine cardiac explants differentiated into fat after several weeks of adipogenic induction. Removal of cardiotrophin-1 (CT) from the fibrosphere growth medium did not improve adipogenesis.

### ***Chondrogenic Differentiation of CDCs***

Two out of six canine CDC cultures tested showed evidence of chondrogenic differentiation, indicated by positive safranin O staining, after several weeks of induction (Figure 19). Of the remaining four cultures, three showed no evidence of cartilage formation, and one was inconclusive. Importantly, control hMSCs undergoing differentiation in parallel with all four of these cultures also showed no evidence of cartilage formation, indicating that the induction media may not have been effective in those experiments. Of the two successfully differentiated cultures, one was derived from cardiospheres grown in the presence of CT, and the other without CT, suggesting no correlation between chondrogenic differentiation and CT.

### ***Osteogenic Differentiation of CDCs***

Six out of six canine RV CDC cultures showed varying degrees of osteogenic differentiation after 2 to 6 weeks of osteogenic induction. The cells stained positively for calcium deposition and showed morphological alterations consistent with osteogenic differentiation (Figure 20). Success of differentiation did not correlate with the presence or absence of CT in the cardiosphere growth medium.

**Figure 19.** Chondrogenic differentiation of canine cardiosphere-derived cells. Differentiation was induced using a standard chondrogenic induction kit, and cell pellets were stained with safranin O. Red staining indicates the presence of proteoglycans, suggestive of cartilage formation. Cytoplasm stains green, and nuclei stain black. Controls were maintained in media without chondrogenic induction and subjected to the same staining protocol. Differentiation of human mesenchymal stem cells cultured in parallel is shown for comparison. Scale bars = 100 $\mu$ m, except for hMSC Control, in which the scale bar is 200 $\mu$ m.

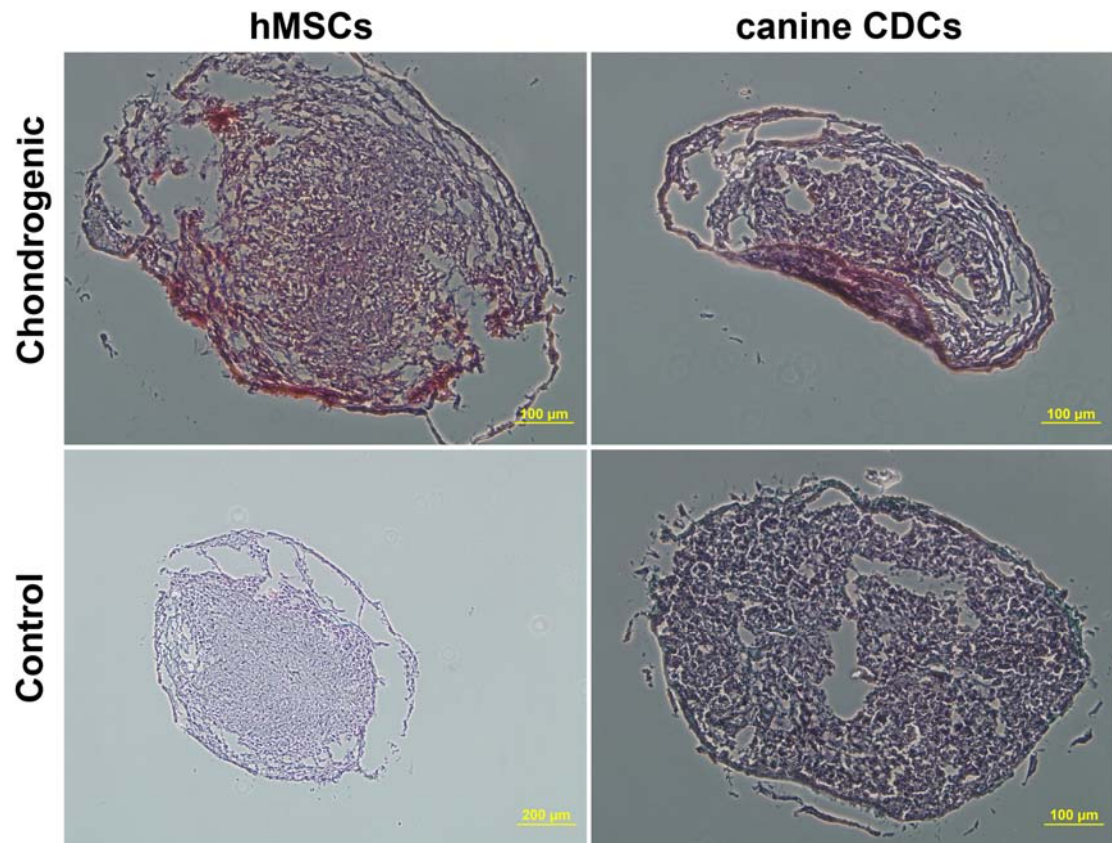
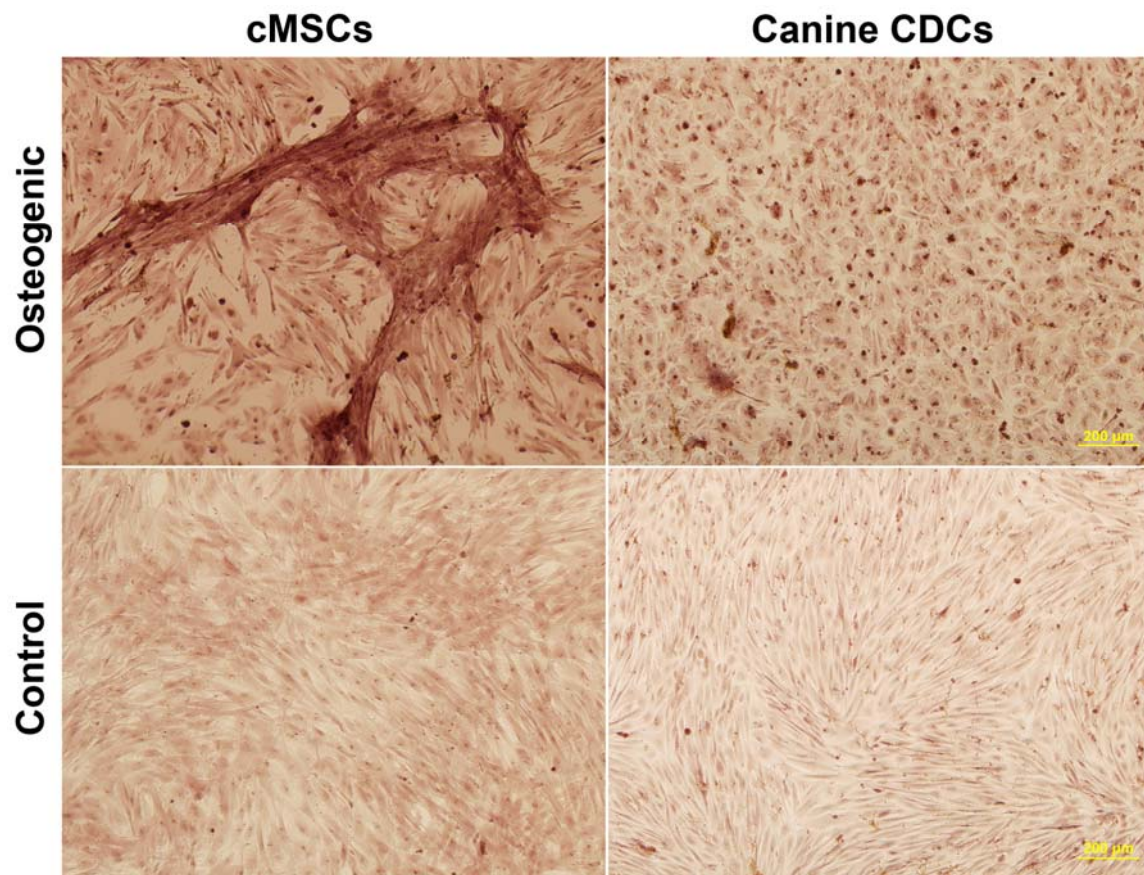


**Figure 20.** Osteogenic differentiation of canine right ventricular CDCs. Red-brown staining indicates calcium deposition. Osteogenically induced CDCs lost the spindle shape typical of fibroblasts and took on a cuboidal morphology consistent with osteoblasts, while control CDCs maintained their fibroblast appearance. Canine mesenchymal stem cells differentiated in parallel are shown for comparison. Controls were cultured in parallel without osteogenic induction and subjected to the same staining protocol. Scale bars = 200 $\mu$ m and apply to all images.



### ***Cardiac Differentiation of Dermal FDCs***

Canine dermal FDCs were co-cultured with rat NRVMs in an attempt to induce cardiac differentiation. Despite several attempts, staining for sarcomeric  $\alpha$ -actinin revealed only rare instances of cardiac differentiation. It was estimated that only 1 in 4000-6000 cells showed any evidence of cardiac differentiation, and in many of these cases, true co-localization of the Dil label used to track the FDCs and sarcomeric  $\alpha$ -actinin was uncertain in Z-stack fluorescent images.

### ***Adipogenic Differentiation of Dermal FDCs***

Adipogenic induction resulted in varying degrees of fat production in 9 out of 10 canine dermal FDC cultures, indicated by positive oil red-O staining (Figure 21). The degree of differentiation was less than ~20% in 5 of the 9 successful cultures. Importantly, the degree of differentiation decreased steadily with successive experiments, suggesting that some change the culture media, supplements, or other factors may be responsible for the decline.

### ***Chondrogenic Differentiation of Dermal FDCs***

One of five canine dermal FDC cultures showed evidence of chondrogenic differentiation, indicated by weakly positive safranin O staining (Figure 22). For three of the four cultures that did not differentiate, human MSCs used as a positive control also failed to differentiate, indicating that the induction procedure may not have been effective in those experiments. The remaining culture that did not differentiate did not have an hMSC culture run in parallel, and a previously cultured hMSC control was used for a staining control. For the culture that did differentiate into cartilage, cardiotrophin-1 was not included in the fibrosphere growth medium. However, this fact alone does not explain the ability of this culture to differentiate into cartilage, as later repeats without cardiotrophin-1 did not differentiate.

### ***Osteogenic Differentiation of Dermal FDCs***

Out of six canine dermal FDC cultures subjected to osteogenic differentiation, four were negative for calcium deposition upon staining, and the other two were inconclusive. The cells in all of these cultures maintained their spindle-shaped morphology, further suggesting that they did not differentiate along a bone lineage.

**Figure 21.** Differentiation of canine dermal FDCs into fat after adipogenic induction. Oil red-O staining; red indicates fat deposits. Differentiation of human MSCs is shown for comparison. Control cells were cultured in parallel without adipogenic induction and were stained using the same protocol. The dermal FDC image is the best example of adipogenic differentiation obtained. Scale bars represent 200 $\mu$ m.



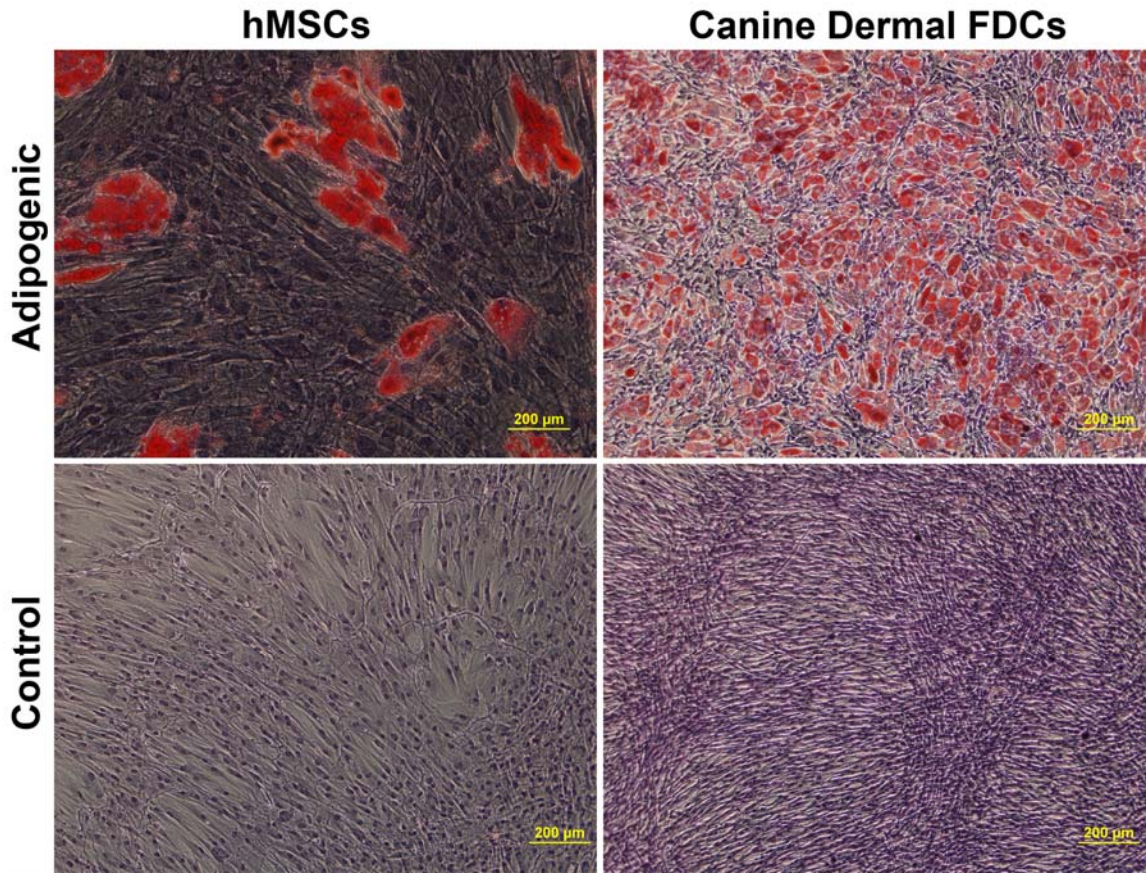
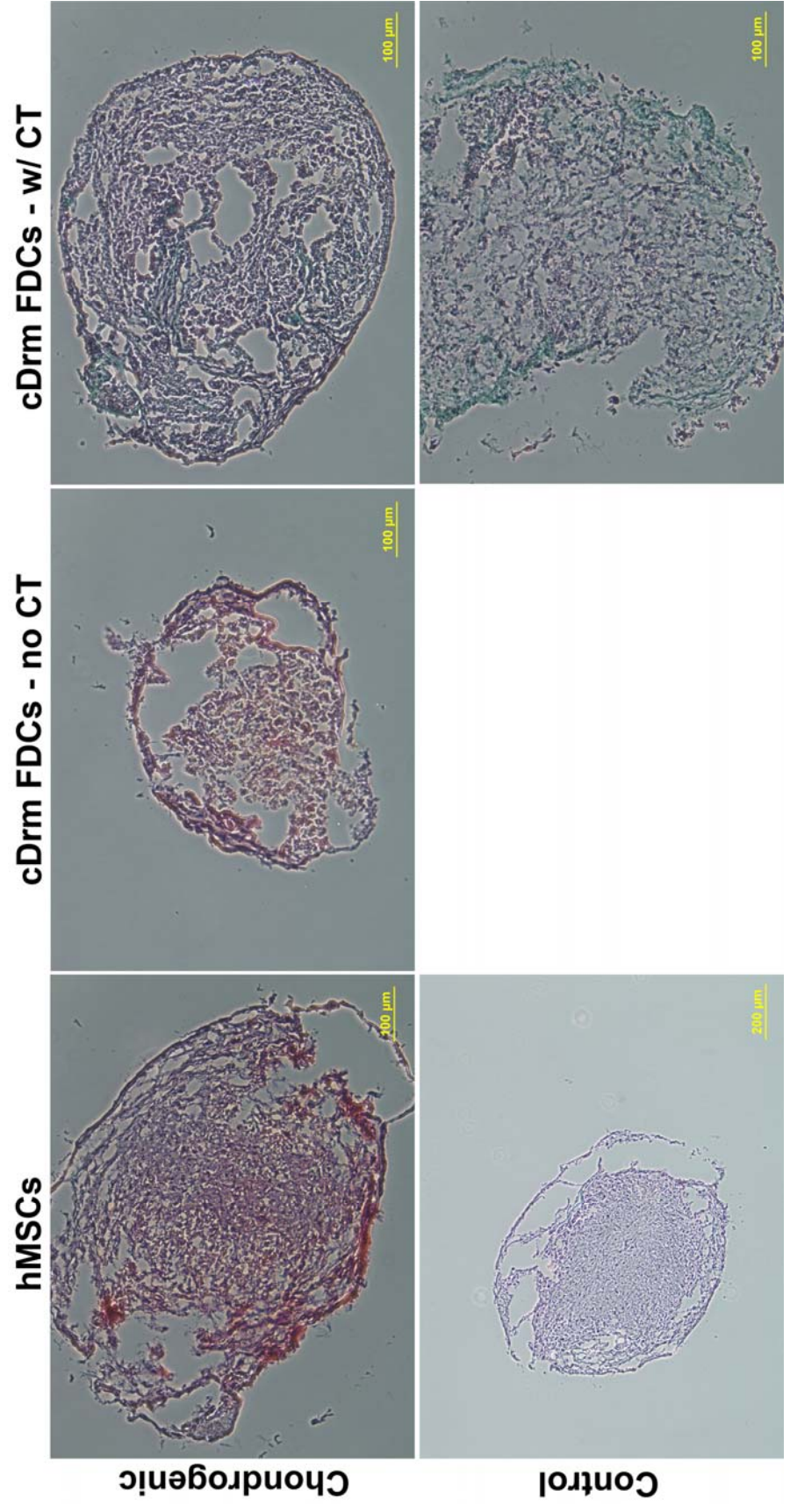


**Figure 22.** Chondrogenic differentiation of canine dermal FDCs. Examples from two different FDC cultures—with and without cardiotrophin-1 (CT) in the fibrosphere growth medium—are shown. Differentiation of hMSCs is shown for comparison. Control samples were cultured in parallel without chondrogenic induction. Due to a low cell yield, a control sample was not available for the “cDrm FDC – no CT” sample. Sections stained with safranin O. Red indicated proteoglycan deposition, suggesting chondrogenic differentiation. Cytoplasm stains green, and nuclei stain black. All staining was performed in parallel, and controls were subjected to the same staining procedure. Although the successfully differentiated culture was derived from fibrospheres grown in the absence of cardiotrophin-1, subsequent repeats without cardiotrophin-1 also failed to differentiate, suggesting that the absence of cardiotrophin-1 alone does not explain the successful differentiation in this culture.



### **Differentiation of Sphere-Forming Cells**

The question remained whether sphere formation was a necessary step in inducing the multipotent potential of the explant-derived cells. To investigate this, differentiation protocols were used on cells taken directly from the explant monolayer without replating on poly-D-lysine-coated plates or exposure to cardiosphere growth medium.

#### ***Cardiac Differentiation of Cardiosphere-Forming Cells***

Canine RV-derived cardiosphere-forming cells (CFCs) were co-cultured with rat NRVMs as done with the CDCs. After 5-6 days of co-culture, multiple examples of sarcomeric  $\alpha$ -actinin in Dil-labeled cells (used to track the CFCs) were found (Figure 23). These cells showed evidence of early sarcomere organization and appeared very similar to the differentiated cells derived from the CDCs.

#### ***Adipogenic and Osteogenic Differentiation of CFCs***

Out of two cultures tested, canine RV-derived CFCs did not differentiate into fat in one and showed a very small amount of adipogenic differentiation in the other. Cells from this same culture were tested for osteogenic differentiation and stained positively for calcium deposition, although the majority of the cells retained their spindle shape.

In another experiment, CFCs were replated in CGM on a culture plate without poly-D-lysine and produced no cardiospheres. The cells were collected after four days and tested for adipogenic and osteogenic differentiation. The osteogenically induced cells stained positively for calcium deposition and showed a bone-like morphology. The cells exposed to adipogenic culture conditions did not differentiate into fat.

#### ***Adipogenic, Chondrogenic, and Osteogenic Differentiation of Dermal Fibrosphere-Forming Cells***

Canine-derived dermal fibrosphere-forming cells (FFCs) were tested for their ability to differentiate into fat, cartilage, and bone. Out of two cultures tested, neither produced fat or bone. One of these was tested for chondrogenic differentiation and failed to become cartilage as well, although positive chondrogenic controls (hMSCs) also failed to differentiate, as described above.

In another experiment, dermal FFCs were replated in CGM on uncoated plates or replated in CEM on poly-D-lysine coated plates for four days. Neither of these conditions promoted sphere formation, and neither of these groups of cells showed adipogenic differentiation. The FFCs plated in CEM on poly-D-lysine did not show

positive staining for calcium deposition, and the cells remained spindle-shaped (Figure 24). The cells plated in CGM on uncoated plates showed positive staining for calcium deposition and a bone-like morphology after six weeks of induction. This was the only dermal-derived culture (with or without sphere formation) to show a bone-like morphology. After only five weeks of osteogenic induction, they stained positively for calcium, but did not have a bone-like morphology.

To investigate whether the fibroblasts would lose the ability to differentiate if maintained in culture in the absence of explant tissue, dermal FFCs were grown for six passages in CEM media. These cells lost the ability to form spheres or to differentiate into fat upon adipogenic induction. To test whether exposure to explant tissue could reactivate them, some were cultured with porcine RV in membrane-separated co-cultures (0.4 $\mu$ m pore size), but these cells also failed to make spheres or differentiate.

#### ***Adipogenic differentiation of NHDFs following growth factor exposure***

NHDFs cultured for 13 days with or without fibronectin and exposure to bFGF, EGF, PDGF, TGF- $\beta$ , or all four growth factors did not form spheres when replated on poly-D-lysine-coated plates in CGM media (described above). Nevertheless, the cells were collected from the poly-D-lysine-coated plates and exposed to adipogenic differentiation media. All of these cells showed evidence of adipogenic differentiation (Figure 25), but the cells grown on fibronectin with all four growth factors differentiated much more successfully than any of the others (Figure 25E).

**Figure 23.** Cardiomyocyte differentiation of canine RV-derived CFCs. A) Image showing Dil label used to track CFCs. Nuclei are blue. B) Staining for sarcomeric  $\alpha$ -actinin (green). C) Overlay showing co-localization of Dil and sarcomeric  $\alpha$ -actinin.

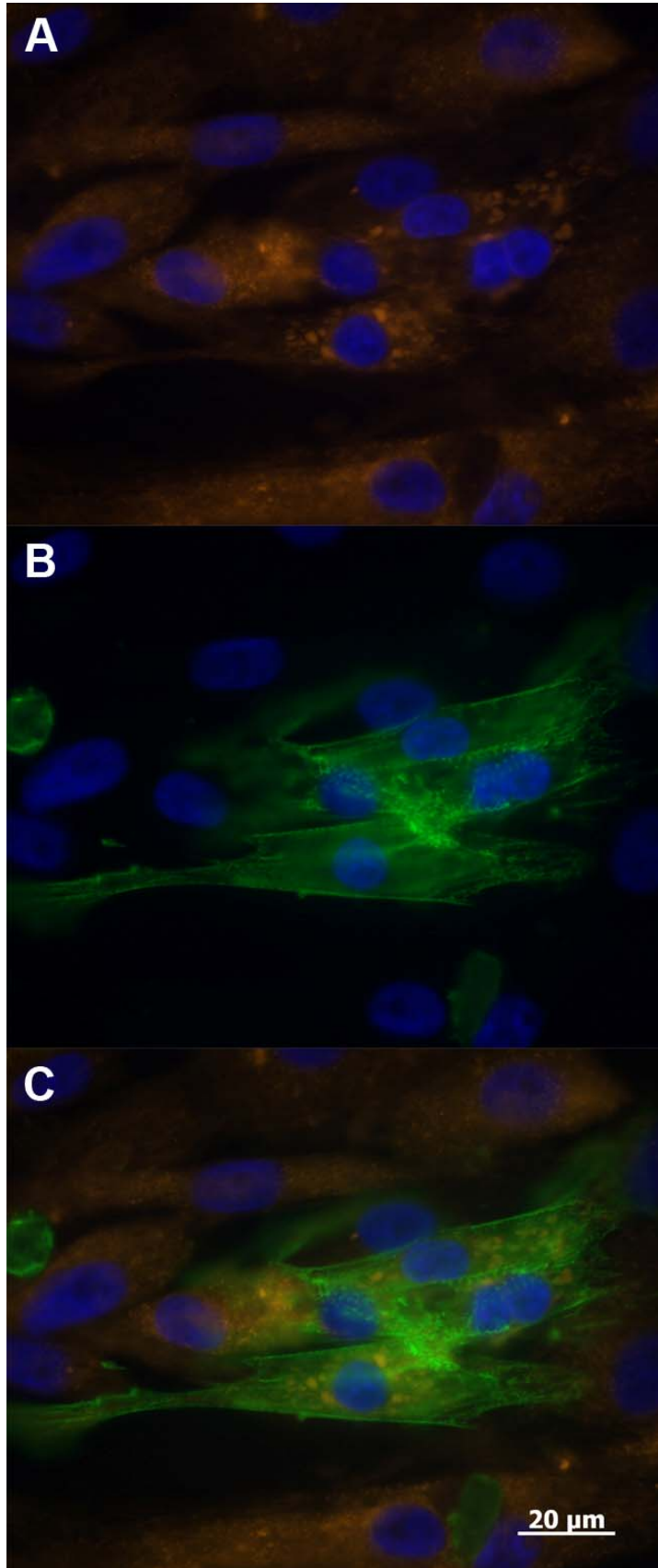


**Figure 24.** Osteogenic differentiation of canine dermal FFCs and FDCs. Canine dermal FFCs were replated in CEM on poly-D-lysine-coated plates, in CGM on poly-D-lysine-coated plates, or in CGM on uncoated plates for four days. The bottom row of images shows that only the cells plated in CGM on poly-D-lysine coated plates formed spheres. Only the FFCs plated in CGM on uncoated plates (top right) showed evidence of calcium deposition in addition to morphological changes consistent with differentiation into bone. Scale bars = 200 $\mu$ m.



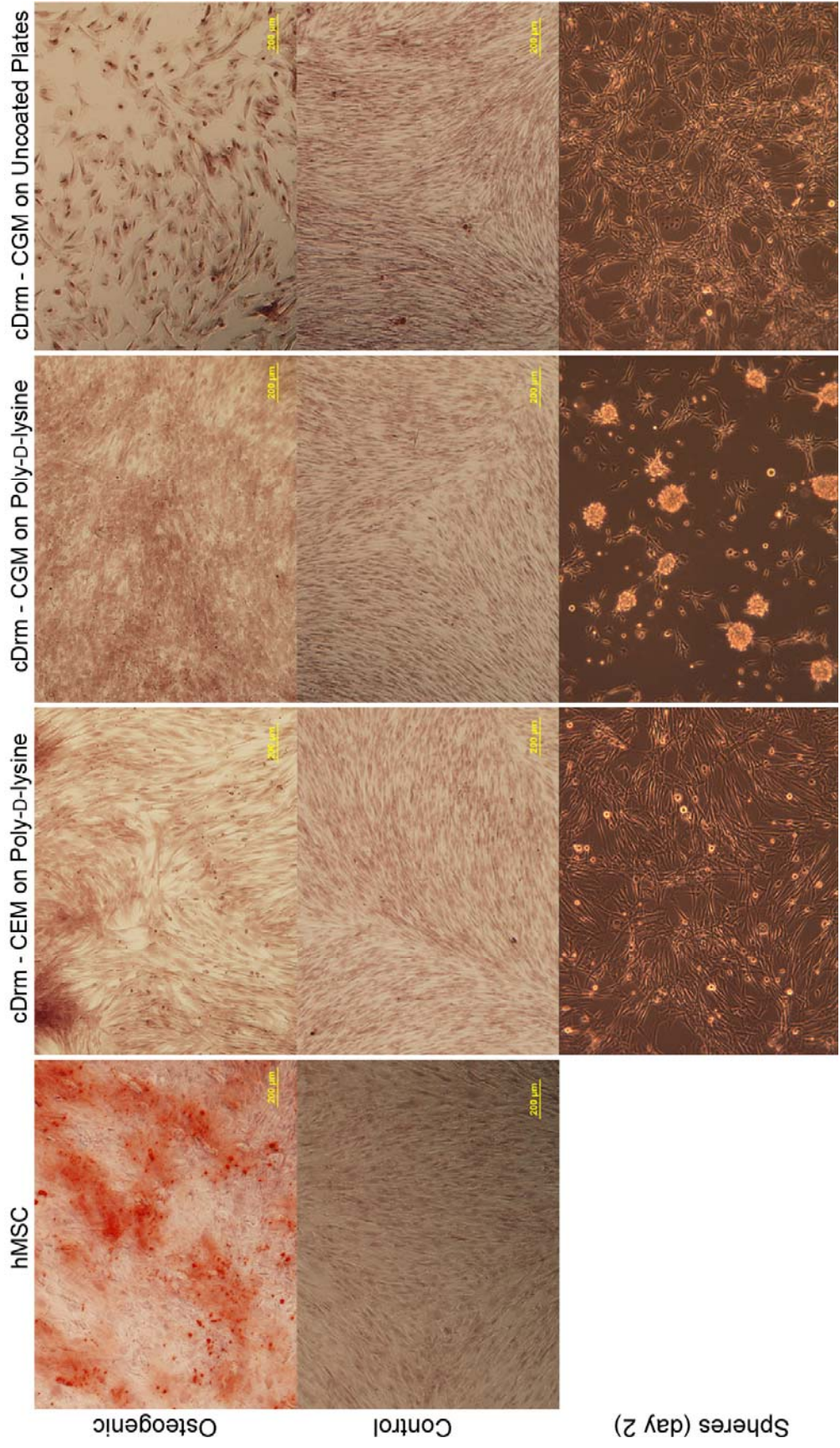
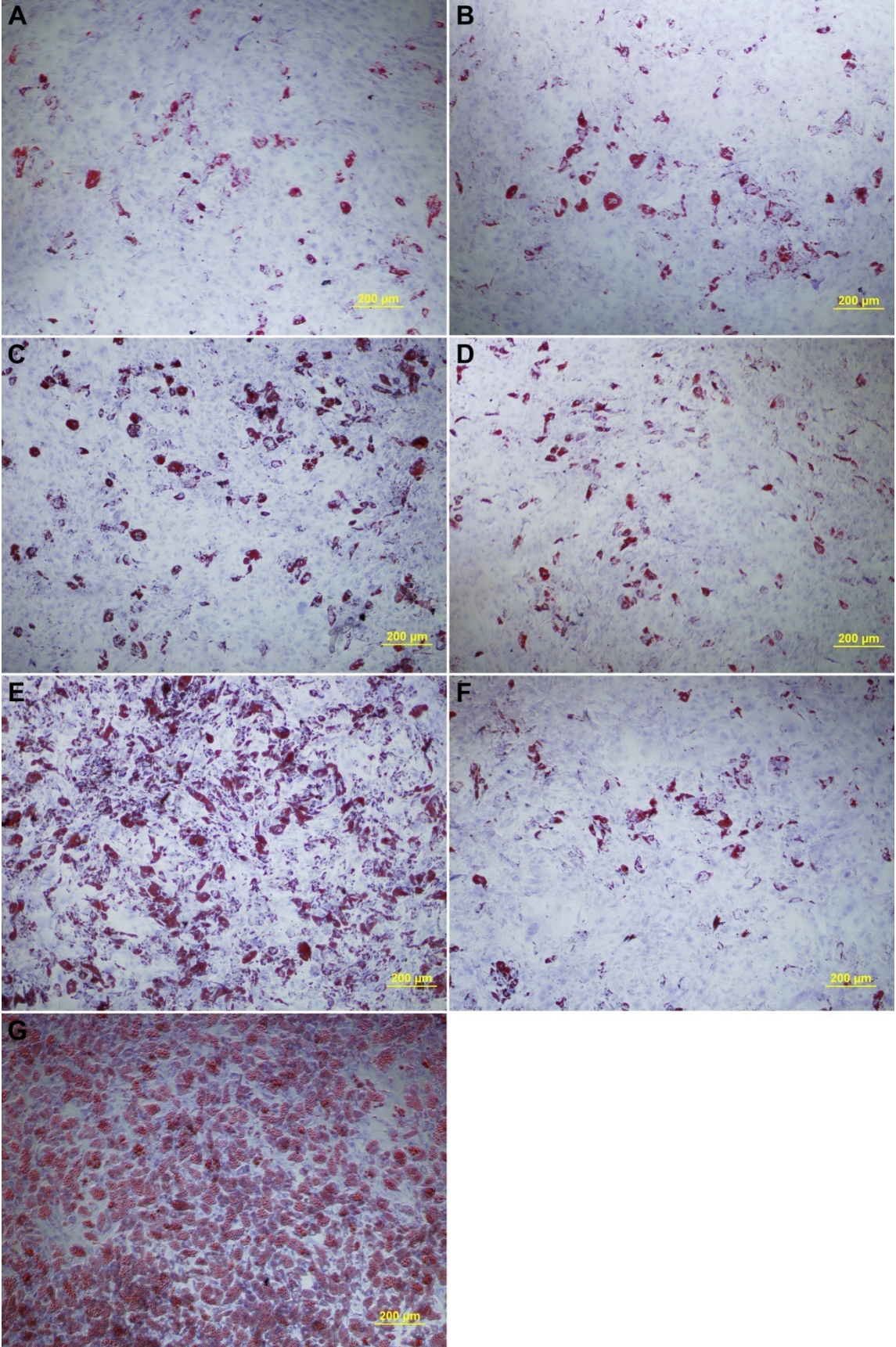


**Figure 25.** Adipogenic differentiation results from NHDFs cultured with or without fibronectin and exposure to growth factors. Oil red-O stained images. A) NHDFs cultured on fibronectin-coated plates and grown in CEM media supplemented with PDGF. B) NHDFs cultured on fibronectin in CEM with TGF- $\beta$ . C) NHDFs cultured on fibronectin in CEM with EGF. D) NHDFs cultured on fibronectin in FBM media (contains bFGF). E) NHDFs cultured on fibronectin in CEM media with PDGF, TGF- $\beta$ , EGF, and bFGF. F) NHDFs cultured without fibronectin in CEM media with PDGF, TGF- $\beta$ , EGF, and bFGF. G) Control hMSCs cultured using standard protocols for hMSC culture and exposed to adipogenic induction media in parallel with the cells in panels A-F. In no instances did controls for each cell type that did not undergo adipogenic induction show any evidence of fat formation.



### 3.2.4 Discussion

#### **Phase-bright cells are derived from the fibroblast layer**

Two papers describe the appearance of “phase-bright” cells in cardiac explant cultures.<sup>28, 29</sup> The investigators claim these cells are a population of cardiac stem cells which can be enriched for based on their poor attachment to poly-D-lysine-coated plates and their tendency to form spheres in suspension culture. Furthermore, they state that these phase-bright cells can be rapidly expanded via sphere formation and can differentiate into cardiac myocytes. The time-lapse recordings of canine and porcine cardiac explants described in the present work unequivocally show phase-bright cells arising from the fibroblast monolayer, undergoing mitosis, and then returning to the monolayer. No phase-bright cells were observed migrating out of the explants across the monolayer and remaining phase-bright indefinitely. These facts, combined with the rapid turnover of the phase bright cells (~2-5 new phase-bright cells appearing per 10× field per hour and many remaining phase-bright for less than an hour), suggests that the phase-bright cell population does not represent a distinct cell population separate from the fibroblasts. Instead, these data suggest that the phase-bright cells are simply fibroblasts undergoing mitosis. Conceptually, this is not a surprising finding when one considers that cytokinesis would likely necessitate that the dividing cell loses its adherence to the culture vessel. In so doing, it would become more spherical and appear phase-bright under phase contrast microscopy (depending on where the focal plane of the microscope is set).

Following these observations, we asked the question “are the phase-bright cells responsible for cardiosphere formation?” Two major pieces of evidence suggest that this is not the case. First, the results showing that the isolated population of phase-bright cells collected without trypsinization of the plate did not form spheres (Figure 10A), while the trypsinized cells from the fibroblast layer left behind did (Figure 10B), suggests that the phase-bright cells are not solely responsible for sphere formation. In a typical culture, the cells collected from the explants were split among six wells when forming spheres. As a result, the phase-bright cell population was split six ways, and cardiospheres formed in all six wells. The fact that no spheres formed when the phase-bright cells were concentrated in one well indicates that these cells do not possess a unique ability to form cardiospheres. The formation of spheres from the fibroblast monolayer cells in the absence of phase-bright cells further supports this. These facts taken together strongly suggest that the vast majority of the cells in the cardiospheres are, in fact, cells from the fibroblast monolayer, rather than enriched phase-bright cells, as the Giacomello<sup>28</sup> and Marban<sup>29</sup> groups suggest. The second piece of evidence comes from the images taken of cardiospheres forming over time (Figure 9). At 4.5 and 26

hours after replating the CFCs on poly-D-lysine-coated plates, the majority of the cells are attached securely to the plate. By 48 hours, the cells have begun to migrate toward one another, grouping themselves into clusters, with several adherent spheres already beginning to form from some of the clusters. At 72 hours, clear cardiosphere formation is apparent, and at 96 hours, very few cells remain on the bottom of the plate. These observations also suggest that the fibroblasts have not been excluded from the spheres; instead, the majority of the cells in the cardiospheres are likely fibroblasts. Attempts were made to confirm the identity of the sphere-forming cells as fibroblasts using immunofluorescent labeling, but none of the six antibodies tested were shown to have specificity for canine or porcine tissue.

There are three possibilities then, regarding the nature of the phase-bright cell population. The first is that they are all dividing fibroblasts with the same degree of plastic potential that the rest of the fibroblasts have. Second is that this population does contain some stem cells as well as fibroblasts, and that both of these subpopulations are undergoing the same process of mitosis. The third possibility is that the phase-bright cells are all fibroblasts, but that they undergo a transient shift to a more plastic state while they are in their phase-bright stage, and that these cells are the ones which undergo differentiation into cardiomyocytes and other cell types. The second and third possibilities can both be addressed by one observation: the osteogenic differentiation of the cardiac-derived cells showing most of the cells undergoing differentiation (Figure 20) suggests that the CDCs do not simply contain a subpopulation of stem cells able to differentiate, nor a “special” fibroblast subpopulation. While stem cells may or may not be present, the high rate of success with osteogenic differentiation indicates that the fibroblasts present in the CDC population also differentiated. Furthermore, concerning the third possibility, we have shown that the phase-bright stage is very short-lived for the majority of the cells in the explant cultures (as little as twenty minutes for some of them). Since four to six days passed between harvest of the CDCs and initiation of the various differentiation protocols, it would seem highly unlikely that any of the phase-bright cells would still be in such a “special” state at the time of differentiation. As a result, it appears most likely that all of the fibroblasts in the explant cultures have more or less the same plastic potential and are capable of differentiation to other mesenchymal lineages.

### **Cells from other tissue sources can form spheres**

Given the evidence that cardiospheres were derived from fibroblasts rather than cardiac stem cells, we wished to determine whether fibroblasts from other tissue sources could also form spheres. Explant cultures from canine and porcine dermis, aorta, and brain were established using the same protocol used for cardiac explant

cultures. Just as with the cardiac explants, a monolayer of fibroblasts appeared from all of these tissue types upon which phase-bright cells could be seen. Time-lapse microscopy confirmed that the phase-bright cells arose from the fibroblast monolayer for all of these tissues, underwent mitosis, and then returned to the monolayer. Cells harvested from all three of these tissue types were able to form spheres (fibrospheres) when cultured under the same conditions as the CFCs. These results further support the notion that sphere formation is not specific to cardiac stem cells and that fibroblasts are the predominant cell type in the spheres.

Purchased primary human fibroblasts (Lonza, Switzerland) from dermal (NHDF) and lung (NHLF) tissue did not form spheres very efficiently on their own, although they did undergo the morphological changes that precede sphere formation in the canine and porcine cells. Rather than forming spheres, the human cells had a tendency to proliferate to near confluence before detaching from the plate. As a result, they lifted off of the plate as one large sheet which pulled into a large three-dimensional mass by the following day. In experiments in which the NHDFs or NHLFs were grown with cardiac explants in membrane-separated (3.0  $\mu\text{m}$  pores) co-cultures, they did form spheres. However, it was noted that fibroblasts from the cardiac explants were able to pass through the 3 $\mu\text{m}$  pores. Nevertheless, the fact that the majority of the cells harvested and used to form spheres were human fibroblasts suggests that the NHDFs and NHLFs are at least capable of participating in the spheres. In a repeated experiment using a membrane with a 0.4 $\mu\text{m}$  pore size, spheres did not form from NHLFs co-cultured with canine LA, although the cells did undergo the morphological changes that precede sphere formation in which they became more spindle-shaped and less flat. The cells also began forming clusters on the bottom of the plate, although the clusters were all interconnected by several cells owing to the high cell density. When the plate was triturated at this stage, many fibrospheres formed (Figure 17B). This suggests an ability of the NHLFs to form spheres, although they may have to be triturated or split to a lower density mid-way through the procedure. It is possible that the culture conditions used by Lonza in preparing their cells and/or the process of cryopreserving the cells for shipping alters their ability to form spheres. This would explain why the NHDFs did not form spheres very efficiently, while the canine and porcine dermal cells we prepared ourselves did.

### **Fibroblasts can differentiate along multiple lineages**

We next sought to confirm whether the CDCs could differentiate into cardiomyocytes in our hands. Toward this end, we attempted a variation on the protocol used by the Marban group<sup>29</sup> in which we co-cultured the CDCs with rat neonatal ventricular myocytes (NRVMs) in segregated areas of the culture plate. After

six days of co-culture, multiple examples of sarcomeric  $\alpha$ -actinin positive CDCs with varying degrees of sarcomeric organization were observed (Figure 18). Although encouraging, we found that the incidence of cardiac differentiation was rather low in these cultures. As a result, we cannot be certain that these cells represent fibroblast differentiation, since we cannot rule out the possibility that the differentiated cells represent a “contaminating” cardiac or mesenchymal stem cell population. Another possible explanation for this observation is that the Dil label used to track the CDCs transferred to some NRVMs, thus causing false positives. However, the fact that co-cultures of the dermal-derived FDCs with NRVMs did not result in significant numbers of Dil<sup>+</sup> cardiomyocytes serves as a good control suggesting that the Dil does not transfer. Furthermore, the occurrence of brightly labeled CDCs lying among NRVMs without dye transfer also suggests that the Dil<sup>+</sup> myocytes are not false positives.

Attempts to differentiate the CDCs to fat were largely unsuccessful, but osteogenic and chondrogenic differentiation was effective. Unlike the results from the NRVM co-cultures, the majority of the cells showed evidence of bone differentiation. This indicates that it was not a subpopulation of stem cells within the cardiospheres which could differentiate into bone, but that the fibroblasts from the spheres actually became bone. Dermal-derived FDCs, on the other hand, differentiated very well into fat (Figure 21), but not bone or cardiomyocytes, and one experiment showed evidence of chondrogenic differentiation. The fact that the adipogenic differentiation was so successful again argues against a small population of stem cells in the dermal fibrospheres that are responsible for the differentiation and suggests that the fibroblasts became fat in these cultures. The differing results from the dermal and cardiac sphere-derived cells suggest that there may be some degree of tissue specificity for differentiation to a given lineage.

Although a novel finding, evidence for differentiation of fibroblasts along other mesenchymal lineages is not without precedent. A 2007 paper by Sudo et al.<sup>51</sup> described the differentiation of cells from purchased primary fibroblast stocks into bone, cartilage, and fat. Despite very highly successful differentiation results, where the majority of the cells appeared to differentiate, the authors attributed their results to a subpopulation of mesenchymal stem cells present in most of their fibroblasts, ignoring the (potentially more plausible) possibility that their fibroblasts themselves differentiated.

### **Is sphere formation a necessary step?**

Cardiosphere-forming cells harvested from canine RV explant plates and directly co-cultured with NRVMs showed an ability to differentiate into cardiomyocytes which

was comparable to that of the CDCs. However, CFCs appeared to be less effective in differentiating into bone than the CDCs, showing evidence of calcium deposition, but failing to take on the cuboidal morphology of bone cells. When the CFCs were exposed to CGM media for four days on regular tissue culture-treated plates (i.e., not poly-D-lysine), they did not form cardiospheres but did differentiate into bone. These cells showed both calcium deposition and a cuboidal morphology typical of osteoblasts.

Dermal fibrosphere-forming cells (FFCs) harvested from dermal explant plates and exposed to adipogenic differentiation media without prior sphere formation did not produce fat. When these cells were exposed to CGM media for four days on tissue culture-treated plates, they, like the CFCs, did not form spheres. These cells failed to differentiate into fat as well, but they did show evidence of osteogenic induction (Figure 24). Interestingly, this was the only dermal-derived cell culture to undergo osteogenic differentiation, suggesting that sphere formation may actually inhibit bone formation with these cells.

NHDFs grown on fibronectin-coated plates in culture media containing the four growth factors EGF, PDGF, bFGF, and TGF- $\beta$  showed a greatly improved ability to differentiate into fat compared to the same cells grown with only one of the four growth factors or all four growth factors without fibronectin. None of these cells formed spheres when exposed to CGM media on poly-D-lysine coated plates.

Taken together, these data suggest that sphere formation is not necessary (possibly even inhibitory) for differentiation to some lineages, but it may be beneficial for some starting cell types. What may be more important than the three-dimensional organization of the cells in culture are the growth factors that the cells are exposed to.

### **Proposed mechanism for fibroblast differentiation and future directions**

We propose that a critical step in inducing fibroblasts to take on a more plastic state is exposure to a tissue injury environment. In all of our experiments, the fibroblasts were collected from minced pieces of tissue kept in culture. This procedure obviously causes a great deal of tissue damage and essentially creates a tissue injury model *in vitro*. It may be that factors released by the injured tissue activate the fibroblasts to participate in injury repair—a known function of fibroblasts. In their activated state, they may gain an ability to differentiate into other cell types which they do not normally have. When fibroblasts are cultured under normal conditions (without pieces of injured tissue present) they would not exhibit such plastic potential. This might explain why purchased fibroblasts, which have likely been passaged without explants present, are less efficient in differentiating into other lineages and why porcine dermal fibroblasts passaged 6 times in the absence of explants completely lose the



ability to differentiate into fat (not shown). Extended passaging of the cells used by Sudo et al.<sup>51</sup> was also shown to decrease differentiation potential. This would further explain why fibroblasts used as controls (presumably purchased cells, although the source is not specified) in the paper by Smith et al.<sup>29</sup> do not appear to repair the infarcted heart as well as the cardiosphere-derived cells, which we have shown are most likely fibroblasts as well.

In line with this proposal is the observation that NHDFs cultured on fibronectin with EGF, PDGF, bFGF, and TGF- $\beta$  were able to differentiate into fat far more effectively than NHDFs cultured in fibroblast media (containing bFGF) or CEM media supplemented with only one of the remaining three factors. These growth factors were chosen as part of an attempt to mimic a tissue injury environment. TGF- $\beta$  has been shown to be a key factor in activation of fibroblasts and their transdifferentiation into myofibroblasts,<sup>52-54</sup> important processes during tissue injury repair. PDGF is released at sites of injury<sup>55</sup> and induces chemotaxis<sup>55</sup> and proliferation<sup>54</sup> of fibroblasts. Fibronectin is known to be important for fibroblast migration and activation during injury repair.<sup>56</sup> Therefore, the improved adipogenic differentiation results obtained with all of these factors may be attributable to a more closely simulated tissue injury environment compared to that of the other culture plates.

Future directions for this research include attempts to fully characterize the factors released during tissue injury and to create more carefully tailored growth media which can activate fibroblasts in the absence of tissue explants. If this can be achieved, it could allow for therapeutic options for expansion and differentiation of a patient's own fibroblasts for repair of heart disease, as well as countless other disorders for which stem cell therapies are currently being investigated. Additionally, patch clamping experiments on the cardiac-differentiated cells should be performed to look for evidence of cardiac-specific currents and the ability to generate an action potential. The CDCs should also be implanted in a myocardial infarction model to see if they can improve cardiac function, as well as implantation into healthy myocardium to see if differentiation into cardiomyocytes occurs *in vivo*.

## 4 References

1. Murry CE, Reinecke H, Pabon LM. Regeneration gaps: observations on stem cells and cardiac repair. *J Am Coll Cardiol*. 2006;47(9):1777-1785.
2. Beltrami CA, Finato N, Rocco M, Feruglio GA, Puricelli C, Cigola E, Quaini F, Sonnenblick EH, Olivetti G, Anversa P. Structural basis of end-stage failure in ischemic cardiomyopathy in humans. *Circulation*. 1994;89(1):151-163.
3. Orlic D, Kajstura J, Chimenti S, Jakoniuk I, Anderson SM, Li B, Pickel J, McKay R, Nadal-Ginard B, Bodine DM, Leri A, Anversa P. Bone marrow cells regenerate infarcted myocardium. *Nature*. 2001;410(6829):701-705.
4. Quaini F, Urbanek K, Beltrami AP, Finato N, Beltrami CA, Nadal-Ginard B, Kajstura J, Leri A, Anversa P. Chimerism of the transplanted heart. *N Engl J Med*. 2002;346(1):5-15.
5. Muller P, Pfeiffer P, Koglin J, Schafers HJ, Seeland U, Janzen I, Urbschat S, Bohm M. Cardiomyocytes of noncardiac origin in myocardial biopsies of human transplanted hearts. *Circulation*. 2002;106(1):31-35.
6. Laflamme MA, Myerson D, Saffitz JE, Murry CE. Evidence for cardiomyocyte repopulation by extracardiac progenitors in transplanted human hearts. *Circ Res*. 2002;90(6):634-640.
7. Bayes-Genis A, Salido M, Sole Ristol F, Puig M, Brossa V, Camprecios M, Corominas JM, Marinosa ML, Baro T, Vela MC, Serrano S, Padro JM, Bayes de Luna A, Cinca J. Host cell-derived cardiomyocytes in sex-mismatch cardiac allografts. *Cardiovasc Res*. 2002;56(3):404-410.
8. Alvarez-Dolado M, Pardal R, Garcia-Verdugo JM, Fike JR, Lee HO, Pfeffer K, Lois C, Morrison SJ, Alvarez-Buylla A. Fusion of bone-marrow-derived cells with Purkinje neurons, cardiomyocytes and hepatocytes. *Nature*. 2003;425(6961):968-973.
9. Beltrami AP, Barlucchi L, Torella D, Baker M, Limana F, Chimenti S, Kasahara H, Rota M, Musso E, Urbanek K, Leri A, Kajstura J, Nadal-Ginard B, Anversa P. Adult cardiac stem cells are multipotent and support myocardial regeneration. *Cell*. 2003;114(6):763-776.
10. Murry CE, Soonpaa MH, Reinecke H, Nakajima H, Nakajima HO, Rubart M, Pasumarthi KBS, Ismail Virag J, Bartelmez SH, Poppa V, Bradford G, Dowell JD, Williams DA, Field LJ. Haematopoietic stem cells do not transdifferentiate into cardiac myocytes in myocardial infarcts. *Nature*. 2004;428(6983):664-668.
11. Balsam LB, Wagers AJ, Christensen JL, Kofidis T, Weissman IL, Robbins RC. Haematopoietic stem cells adopt mature haematopoietic fates in ischaemic myocardium. *Nature*. 2004;428(6983):668-673.
12. Laflamme MA, Murry CE. Regenerating the heart. *Nat Biotechnol*. 2005;23(7):845-856.
13. Makino S, Fukuda K, Miyoshi S, Konishi F, Kodama H, Pan J, Sano M, Takahashi T, Hori S, Abe H, Hata J-i, Umezawa A, Ogawa S. Cardiomyocytes can be generated from marrow stromal cells in vitro. *J Clin Invest*. 1999;103(5):697-705.

14. Bittira B, Kuang JQ, Al-Khaldi A, Shum-Tim D, Chiu RC. In vitro preprogramming of marrow stromal cells for myocardial regeneration. *Ann Thorac Surg*. 2002;74(4):1154-1159; discussion 1159-1160.
15. Toma C, Pittenger MF, Cahill KS, Byrne BJ, Kessler PD. Human mesenchymal stem cells differentiate to a cardiomyocyte phenotype in the adult murine heart. *Circulation*. 2002;105(1):93-98.
16. Shake JG, Gruber PJ, Baumgartner WA, Senechal G, Meyers J, Redmond JM, Pittenger MF, Martin BJ. Mesenchymal stem cell implantation in a swine myocardial infarct model: engraftment and functional effects. *The Annals of Thoracic Surgery*. 2002;73(6):1919-1926.
17. Ma J, Ge J, Zhang S, Sun A, Shen J, Chen L, Wang K, Zou Y. Time course of myocardial stromal cell-derived factor 1 expression and beneficial effects of intravenously administered bone marrow stem cells in rats with experimental myocardial infarction. *Basic Res Cardiol*. 2005;100(3):217-223.
18. Kajstura J, Leri A, Finato N, Di Loreto C, Beltrami CA, Anversa P. Myocyte proliferation in end-stage cardiac failure in humans. *PNAS*. 1998;95(15):8801-8805.
19. Beltrami AP, Urbanek K, Kajstura J, Yan S-M, Finato N, Bussani R, Nadal-Ginard B, Silvestri F, Leri A, Beltrami CA, Anversa P. Evidence that human cardiac myocytes divide after myocardial infarction. *N Engl J Med*. 2001;344(23):1750-1757.
20. Pasumarthi KBS, Field LJ. Cardiomyocyte cell cycle regulation. *Circ Res*. 2002;90(10):1044-1054.
21. Poss KD, Wilson LG, Keating MT. Heart regeneration in zebrafish. *Science*. 2002;298(5601):2188-2190.
22. Schuster MD, Kocher AA, Seki T, Martens TP, Xiang G, Homma S, Itescu S. Myocardial neovascularization by bone marrow angioblasts results in cardiomyocyte regeneration. *Am J Physiol Heart Circ Physiol*. 2004;287(2):H525-532.
23. Zevitz ME. Heart Failure. *eMedicine.com*; 2005:<http://www.emedicine.com/med/topic3552.htm>.
24. American Heart Association. *Heart Disease and Stroke Statistics—2005 Update*. Dallas, Texas: ©2005, American Heart Association; 2005.
25. Levy D, Kenchaiah S, Larson MG, Benjamin EJ, Kupka MJ, Ho KKL, Murabito JM, Vasan RS. Long-term trends in the incidence of and survival with heart failure. *N Engl J Med*. 2002;347(18):1397-1402.
26. Bonow RO, Smaha LA, Smith SC, Jr., Mensah GA, Lenfant C. World heart day 2002: the international burden of cardiovascular disease: responding to the emerging global epidemic. *Circulation*. 2002;106(13):1602-1605.
27. American Heart Association. *Heart Disease and Stroke Statistics—2008 Update*. Dallas, Texas: ©2005, American Heart Association; 2008.
28. Messina E, De Angelis L, Frati G, Morrone S, Chimenti S, Fiordaliso F, Salio M, Battaglia M, Latronico MVG, Coletta M, Vivarelli E, Frati L, Cossu G, Giacomello A. Isolation and expansion of adult cardiac stem cells from human and murine heart. *Circ Res*. 2004;95(9):911-921.

29. Smith RR, Barile L, Cho HC, Leppo MK, Hare JM, Messina E, Giacomello A, Abraham MR, Marban E. Regenerative potential of cardiosphere-derived cells expanded from percutaneous endomyocardial biopsy specimens. *Circulation*. 2007;115(7):896-908.
30. Doronin SV, Kochupura PV, Azeloglu EU, Kelly DJ, Potapova IA, Zuckerman J, Cohen IS, Gaudette GR. Canine heart regeneration. Paper presented at: 2005 Keystone Symposia: Molecular Biology of Cardiac Diseases and Regeneration; April 3-8, 2005; Steamboat Springs, CO.
31. Fraidenraich D, Stillwell E, Romero E, Wilkes D, Manova K, Basson CT, Benezra R. Rescue of cardiac defects in Id knockout embryos by injection of embryonic stem cells. *Science*. 2004;306(5694):247-252.
32. Zygmunt AC. Intracellular calcium activates a chloride current in canine ventricular myocytes. *Am J Physiol Heart Circ Physiol*. 1994;267(5):H1984-1995.
33. Doronin SV, Kelly DJ, Schuldt AJ, Potapova IA, Rosen AB, Brink PR, Cohen IS, Gaudette GR. Stem cells induce myocardial proliferation in vivo and in vitro by release of paracrine factors. Paper presented at: Keystone Symposia: Molecular Pathways in Cardiac Development and Disease/Integrative Basis of Cardiovascular Disease; Jan 22-27, 2007; Breckenridge, CO.
34. Nusse R. Wnt signaling in disease and in development. *Cell Res*. 2005;15(1):28-32.
35. Engel FB, Schebesta M, Duong MT, Lu G, Ren S, Madwed JB, Jiang H, Wang Y, Keating MT. p38 MAP kinase inhibition enables proliferation of adult mammalian cardiomyocytes. *Genes Dev*. 2005;19(10):1175-1187.
36. Singer KH, Scarce RM, Tuck DT, Whichard LP, Denning SM, Haynes BF. Removal of fibroblasts from human epithelial cell cultures with use of a complement fixing monoclonal antibody reactive with human fibroblasts and monocytes/macrophages. *J Invest Dermatol*. 1989;92(2):166-170.
37. Hertig CM, Kubalak SW, Wang Y, Chien KR. Synergistic roles of neuregulin-1 and insulin-like growth factor-I in activation of the phosphatidylinositol 3-kinase pathway and cardiac chamber morphogenesis. *J. Biol. Chem*. 1999;274(52):37362-37369.
38. Reiss K, Cheng W, Ferber A, Kajstura J, Li P, Li B, Olivetti G, Homcy CJ, Baserga R, Anversa P. Overexpression of insulin-like growth factor-1 in the heart is coupled with myocyte proliferation in transgenic mice. *Proceedings of the National Academy of Sciences*. 1996;93(16):8630-8635.
39. McMullen JR, Shioi T, Huang W-Y, Zhang L, Tarnavski O, Bisping E, Schinke M, Kong S, Sherwood MC, Brown J, Riggi L, Kang PM, Izumo S. The insulin-like growth factor 1 receptor induces physiological heart growth via the phosphoinositide 3-kinase(p110{alpha}) pathway. *J. Biol. Chem*. 2004;279(6):4782-4793.
40. Schuldt AJ, Rosen MR, Gaudette GR, Cohen IS. Repairing damaged myocardium: evaluating cells used for cardiac regeneration. *Curr Treat Options Cardiovasc Med*. 2008;10(1):59-72.
41. Mauro A. Satellite cell of skeletal muscle fibers. *J. Cell Biol*. 1961;9(2):493-495.

42. Schmalbruch H, Hellhammer U. The number of satellite cells in normal human muscle. *Anat Rec.* 1976;185(3):279-287.
43. Dawn B, Stein AB, Urbanek K, Rota M, Whang B, Rastaldo R, Torella D, Tang XL, Rezazadeh A, Kajstura J, Leri A, Hunt G, Varma J, Prabhu SD, Anversa P, Bolli R. Cardiac stem cells delivered intravascularly traverse the vessel barrier, regenerate infarcted myocardium, and improve cardiac function. *Proc Natl Acad Sci U S A.* 2005;102(10):3766-3771.
44. Oh H, Bradfute SB, Gallardo TD, Nakamura T, Gaussin V, Mishina Y, Pocius J, Michael LH, Behringer RR, Garry DJ, Entman ML, Schneider MD. Cardiac progenitor cells from adult myocardium: homing, differentiation, and fusion after infarction. *Proc Natl Acad Sci U S A.* 2003;100(21):12313-12318.
45. Martin CM, Meeson AP, Robertson SM, Hawke TJ, Richardson JA, Bates S, Goetsch SC, Gallardo TD, Garry DJ. Persistent expression of the ATP-binding cassette transporter, *Abcg2*, identifies cardiac SP cells in the developing and adult heart. *Dev Biol.* 2004;265(1):262-275.
46. Laugwitz K-L, Moretti A, Lam J, Gruber P, Chen Y, Woodard S, Lin L-Z, Cai C-L, Lu MM, Reth M, Platoshyn O, Yuan JXJ, Evans S, Chien KR. Postnatal isl1+ cardioblasts enter fully differentiated cardiomyocyte lineages. *Nature.* 2005;433(7026):647-653.
47. Pfister O, Mouquet F, Jain M, Summer R, Helmes M, Fine A, Colucci WS, Liao R. CD31- but not CD31+ cardiac side population cells exhibit functional cardiomyogenic differentiation. *Circ Res.* 2005;97(1):52-61.
48. Wang X, Hu Q, Nakamura Y, Lee J, Zhang G, From AHL, Zhang J. The role of the Sca-1+/CD31- cardiac progenitor cell population in postinfarction left ventricular remodeling. *Stem Cells.* 2006;24(7):1779-1788.
49. Murry CE, Reinecke H, Pabon LM. Regeneration gaps: observations on stem cells and cardiac repair. *Journal of the American College of Cardiology.* 2006;47(9):1777-1785.
50. Bien H, Yin L, Entcheva E. Cardiac cell networks on elastic microgrooved scaffolds. *IEEE Eng Med Biol Mag.* 2003;22(5):108-112.
51. Sudo K, Kanno M, Miharada K, Ogawa S, Hiroyama T, Saijo K, Nakamura Y. Mesenchymal progenitors able to differentiate into osteogenic, chondrogenic, and/or adipogenic cells in vitro are present in most primary fibroblast-like cell populations. *Stem Cells.* 2007;25(7):1610-1617.
52. Narine K, Wever OD, Valckenborgh DV, Francois K, Bracke M, Desmet S, Mareel M, Nooten GV. Growth factor modulation of fibroblast proliferation, differentiation, and invasion: implications for tissue valve engineering. *Tissue Engineering.* 2006;12(10):2707-2716.
53. Rahimi RA, Leof EB. TGF-beta signaling: a tale of two responses. *J Cell Biochem.* 2007;102(3):593-608.
54. Desmouliere A, Geinoz A, Gabbiani F, Gabbiani G. Transforming growth factor-beta 1 induces alpha-smooth muscle actin expression in granulation tissue myofibroblasts and in quiescent and growing cultured fibroblasts. *J. Cell Biol.* 1993;122(1):103-111.

55. Lin F, Ren X-D, Doris G, Clark RAF. Three-dimensional migration of human adult dermal fibroblasts from collagen lattices into fibrin/fibronectin gels requires syndecan-4 proteoglycan. *J Invest Dermatol*. 2005;124(5):906-913.
56. Ghosh K, Ren X-D, Shu XZ, Prestwich GD, Clark RAF. Fibronectin functional domains coupled to hyaluronan stimulate adult human dermal fibroblast responses critical for wound healing. *Tissue Engineering*. 2006;12(3):601-613.